NK cell–derived GM-CSF potentiates inflammatory arthritis and is negatively regulated by CIS

Cynthia Louis, Fernando Souza-Fonseca-Guimaraes, Yuyan Yang, Damian D'silva, Tobias Kratina, Laura Dagley, Soroor Hediyeh-Zadeh, Jai Rautela, Seth Lucian Masters, Melissa Davis, et al.

JEM Journal of Experimental Medicine

ARTICLE

NK cell–derived GM-CSF potentiates inflammatory arthritis and is negatively regulated by CIS

Cynthia Louis[1,2*], Fernando Souza-Fonseca-Guimaraes[2,3,4*], Yuyan Yang[1,2], Damian D'Silva[1,2], Tobias Kratina[2,3], Laura Dagley[2,5], Soroor Hediyeh-Zadeh[2,6], Jai Rautela[2,3,7], Seth Lucian Masters[1,2], Melissa J. Davis[2,6], Jeffrey J. Babon[2,8], Bogoljub Ciric[9], Eric Vivier[10,11,12], Warren S. Alexander[2,13], Nicholas D. Huntington[2,7**], and Ian P. Wicks[1,2,14**]

Despite increasing recognition of the importance of GM-CSF in autoimmune disease, it remains unclear how GM-CSF is regulated at sites of tissue inflammation. Using GM-CSF fate reporter mice, we show that synovial NK cells produce GM-CSF in autoantibody-mediated inflammatory arthritis. Synovial NK cells promote a neutrophilic inflammatory cell infiltrate, and persistent arthritis, via GM-CSF production, as deletion of NK cells, or specific ablation of GM-CSF production in NK cells, abrogated disease. Synovial NK cell production of GM-CSF is IL-18–dependent. Furthermore, we show that cytokine-inducible SH2-containing protein (CIS) is crucial in limiting GM-CSF signaling not only during inflammatory arthritis but also in experimental allergic encephalomyelitis (EAE), a murine model of multiple sclerosis. Thus, a cellular cascade of synovial macrophages, NK cells, and neutrophils mediates persistent joint inflammation via production of IL-18 and GM-CSF. Endogenous CIS provides a key brake on signaling through the GM-CSF receptor. These findings shed new light on GM-CSF biology in sterile tissue inflammation and identify several potential therapeutic targets.

Introduction

Rheumatoid arthritis (RA) is a chronic inflammatory disease that targets synovial joints. The pathology of RA includes the generation of autoantibodies and persistent cytokine dysregulation. It has become clear that the cytokine GM-CSF (CSF2) plays an important role in RA as well as other autoimmune diseases (Becher et al., 2016; Wicks and Roberts, 2016). GM-CSF–deficient mice have attenuated collagen-induced arthritis (CIA, a murine model of RA) and experimental autoimmune encephalomyelitis (EAE, a murine model for multiple sclerosis [MS]; Campbell et al., 1998; McQualter et al., 2001). Recent clinical trials confirm the benefit of GM-CSF antagonism on established disease in RA (Burmester et al., 2017, 2018). However, how GM-CSF is regulated at sites of tissue inflammation is not well understood.

GM-CSF can be produced by a number of cell types, depending on the inflammatory context. GM-CSF–producing T helper (Th) type 17 cells have been identified in the arthritic joints of autoimmune SKG mice, a strain that carries a point mutation in the gene encoding the TCR-proximal signaling molecule ZAP-70 (Hirota et al., 2018). Synovial fibroblasts and type 2 innate lymphoid cells (ILC) were also identified as GM-CSF producers, induced by IL-17 or damage-associated molecular patterns, respectively (Hirota et al., 2018). In the EAE model of MS, GM-CSF confers pathogenicity on the $CD4^+$ Th17 cell subset (Codarri et al., 2011; El-Behi et al., 2011; Komuczki et al., 2019), which in turn primes an encephalitogenic phenotype in $Ly6C^+$ monocytes (Croxford et al., 2015). GM-CSF–producing $CD4^+$ T cells have been identified in cerebrospinal fluid of MS patients (Noster et al., 2014) and in the synovium of RA patients (Reynolds et al., 2016). However, GM-CSF production is not restricted to these cells. Other sources include innate response activator B cells during sepsis (Rauch et al., 2012), cardiac

[1]Inflammation Division, The Walter and Eliza Hall Institute of Medical Research, Parkville, Australia; [2]Medical Biology, University of Melbourne, Parkville, Australia; [3]Molecular Immunology Division, The Walter and Eliza Hall Institute of Medical Research, Parkville, Australia; [4]University of Queensland Diamantina Institute, Translational Research Institute, Brisbane, Australia; [5]Systems Biology and Personalized Medicine Division, The Walter and Eliza Hall Institute of Medical Research, Parkville, Australia; [6]Bioinformatics Division, The Walter and Eliza Hall Institute of Medical Research, Parkville, Australia; [7]Biomedicine Discovery Institute and the Department of Biochemistry and Molecular Biology, Monash University, Clayton, Australia; [8]Structural Biology Division, The Walter and Eliza Hall Institute of Medical Research, Parkville, Australia; [9]Department of Neurology, Thomas Jefferson University. Philadelphia, PA; [10]Innate Pharma Research Labs, Innate Pharma, Marseille, France; [11]Aix Marseille University, CNRS, INSERM, CIML, Marseille, France; [12]Service d'Immunologie, Marseille Immunopole, Hôpital de la Timone, Assistance Publique-Hôpitaux de Marseille, Marseille, France; [13]Blood Cells and Blood Cancer Division, The Walter and Eliza Hall Institute of Medical Research, Parkville, Australia; [14]Rheumatology Unit, Royal Melbourne Hospital, Parkville, Australia.

*C. Louis and F. Souza-Fonseca-Guimaraes contributed equally to this paper; **N.D. Huntington and I.P. Wicks contributed equally to this paper; Correspondence to Cynthia Louis: louis.c@wehi.edu.au; Ian P. Wicks: wicks@wehi.edu.au.

fibroblasts in myocardial infarction and coronary vasculitis (Anzai et al., 2017; Stock et al., 2016), and natural killer (NK) cells during systemic *Candida albicans* infection (Bär et al., 2014; Domínguez-Andrés et al., 2017). Thus, GM-CSF can be produced by hematopoietic and/or nonhematopoietic cells, depending on the inflammatory context and environmental triggers.

RA is associated with a number of autoantibodies (e.g., anti-cyclic citrullinated peptide antibodies, rheumatoid factor), and these predict more severe disease (Smolen et al., 2016; Syversen et al., 2008). The serum transfer-induced arthritis (STIA) model has been widely used to study the effector phase of autoantibody-mediated arthritis (Korganow et al., 1999; Monach et al., 2008). GM-CSF contributes to STIA independently of adaptive immune cells (Cook et al., 2011). However, how GM-CSF is regulated in this clinically relevant context remains to be defined. Neutrophils and macrophages are the major cells in the inflammatory infiltrate in the STIA model (Ji et al., 2002a), but other innate immune cells, such as mast cells and NK cells, have also been reported (Nigrovic and Lee, 2007; Söderström et al., 2010). Little is known about whether, and how, these accessory cells impact on the course of joint inflammation.

NK cells are a subset of ILCs, with antitumoral and antiviral functions (Vivier et al., 2011; Vivier et al., 2018). NK cells have been hypothesized to promote antibody-mediated autoimmunity through engagement of FcγRIIIa/CD16, as well as their natural cytotoxicity receptors (NCR), and to activate myeloid cells via cytokine production (Schleinitz et al., 2010). NK-derived IFN-γ has been linked to more severe RA (Dalbeth and Callan, 2002; Pridgeon et al., 2003; Yamin et al., 2019), but the role of IFN-γ and NK cells in experimental models of arthritis remains controversial. IFN-$\gamma^{-/-}$ mice developed more severe CIA (Guedez et al., 2001), and there are conflicting reports on the effect of NK cell depletion in the CIA model (Lo et al., 2008; Söderström et al., 2010). Thus, although it is known that immature, noncytotoxic, cytokine-producing NK cells are present in the inflamed synovium of arthritis patients (Dalbeth and Callan, 2002; Pridgeon et al., 2003; Yamin et al., 2019), whether and how these synovial NK cells contribute to the course of arthritis remain to be investigated.

GM-CSF signaling primes myeloid cells for developmental and pro-inflammatory functions. GM-CSF signaling is mediated through the heterodimeric GM-CSF receptor (GM-CSFRα, a specific, low-affinity ligand-binding subunit) and the common signaling β (GM-CSFRβ) signal-transducing subunit, which is shared with the IL-3 and IL-5 receptors. The suppressor of cytokine signaling (SOCS) proteins (cytokine-inducible SH2-containing protein [CIS], SOCS1-7) are cytokine-inducible negative regulators that limit cytokine signaling. SOCS family proteins possess a central SH2 domain (which binds to phosphorylated tyrosine motifs in target proteins) and a C-terminal SOCS box that mediates the formation of an E3 ubiquitin ligase complex to ubiquitinate SOCS-interacting proteins for proteasomal degradation (Morris et al., 2018). Although a number of SOCS family members have been proposed (Bunda et al., 2013; Esashi et al., 2008; Jackson et al., 2004), whether GM-CSF signaling induces direct, stimulus-induced negative regulation has not been resolved (Wicks and Roberts, 2016).

In this report, we addressed two related aspects of GM-CSF biology in the context of autoantibody-mediated inflammatory arthritis. Using gene reporter mice, we identified NK cells as a major cellular source of GM-CSF production in STIA. We found that mice with genetic or pharmacologic depletion of NK cells still developed arthritis, but had markedly reduced disease progression. To address if NK-derived GM-CSF contributes to STIA, we generated a *Csf2*$^{fl/fl}$ transgenic mouse line to allow specific GM-CSF deletion. Deletion of GM-CSF in NK cells was sufficient to suppress the progression of STIA. We also found that GM-CSF production by synovial NK cells was regulated by IL-18. Furthermore, we validated CIS as a key suppressor of GM-CSF signaling. Loss of CIS resulted in prolonged GM-CSF–driven JAK-STAT signaling in myeloid cells, and in keeping with these observations, CIS-deficient mice had exacerbated STIA. We provide evidence for altered recycling of GM-CSFRβ in the absence of CIS. In summary, synovial NK cells can propagate antibody-mediated joint inflammation via GM-CSF production, following activation by IL-18. We show that the SOCS family member CIS is a direct, stimulus-induced negative regulator of GM-CSF signaling in myeloid cells. These findings shed new light on how GM-CSF mediates autoimmune tissue inflammation and reveal several new potential therapeutic targets.

Results

GM-CSF is produced by NK cells during autoantibody-mediated arthritis

GM-CSF production is required for CIA (Campbell et al., 1998) and STIA (Cook et al., 2011). Previous studies have highlighted the production of GM-CSF by diverse cell types, including CD4$^+$ Th17 cells, tissue fibroblasts, and most recently, type 2 ILCs (Anzai et al., 2017; Hirota et al., 2018; Stock et al., 2016). It is unknown which cells produce this pro-inflammatory cytokine during T cell–independent, autoantibody-mediated STIA. We used a GM-CSF reporter/fate reporter (Gr/fr) mouse system (Fig. S1 A) to monitor GM-CSF expression at the single-cell level. Briefly, this transgenic construct reports expression of GM-CSF, driven by the physiological control elements for the *Csf2* gene. GM-CSF expression triggers expression of both iCre and blue fluorescent protein (BFP). These mice were crossed to Rosa26eYFP mice to generate Gr/fr mice that also enable lineage tracing via iCre-mediated YFP expression. Hence, cells expressing GM-CSF in real time can be identified as BFP$^+$ YFP$^+$, while BFP$^-$ YFP$^+$ marked cells have ceased to express GM-CSF. To validate this system, we verified a BFP$^+$ YFP$^+$ population in Th17-polarized splenocytes (Fig. S1 B). Furthermore, a CD45$^-$ BFP$^+$ YFP$^+$ population was identified in the lung, most likely representing gp38$^-$ epithelial cells and gp38$^+$ fibroblasts (Fig. S1 C), which are known producers of GM-CSF in the normal lung (Guilliams et al., 2013).

Unlike WT mice, the GM-CSF–producing BFP$^+$ YFP$^+$ population was readily apparent in the joints of Gr/fr mice with STIA (Fig. 1 A), which were distinct from autofluorescent (YFP$^-$) synovial exudate cells observed in both WT and Gr/fr mice. The frequency of GM-CSF–producing BFP$^+$ cells in the synovium paralleled the clinical progression of STIA, which increases up to

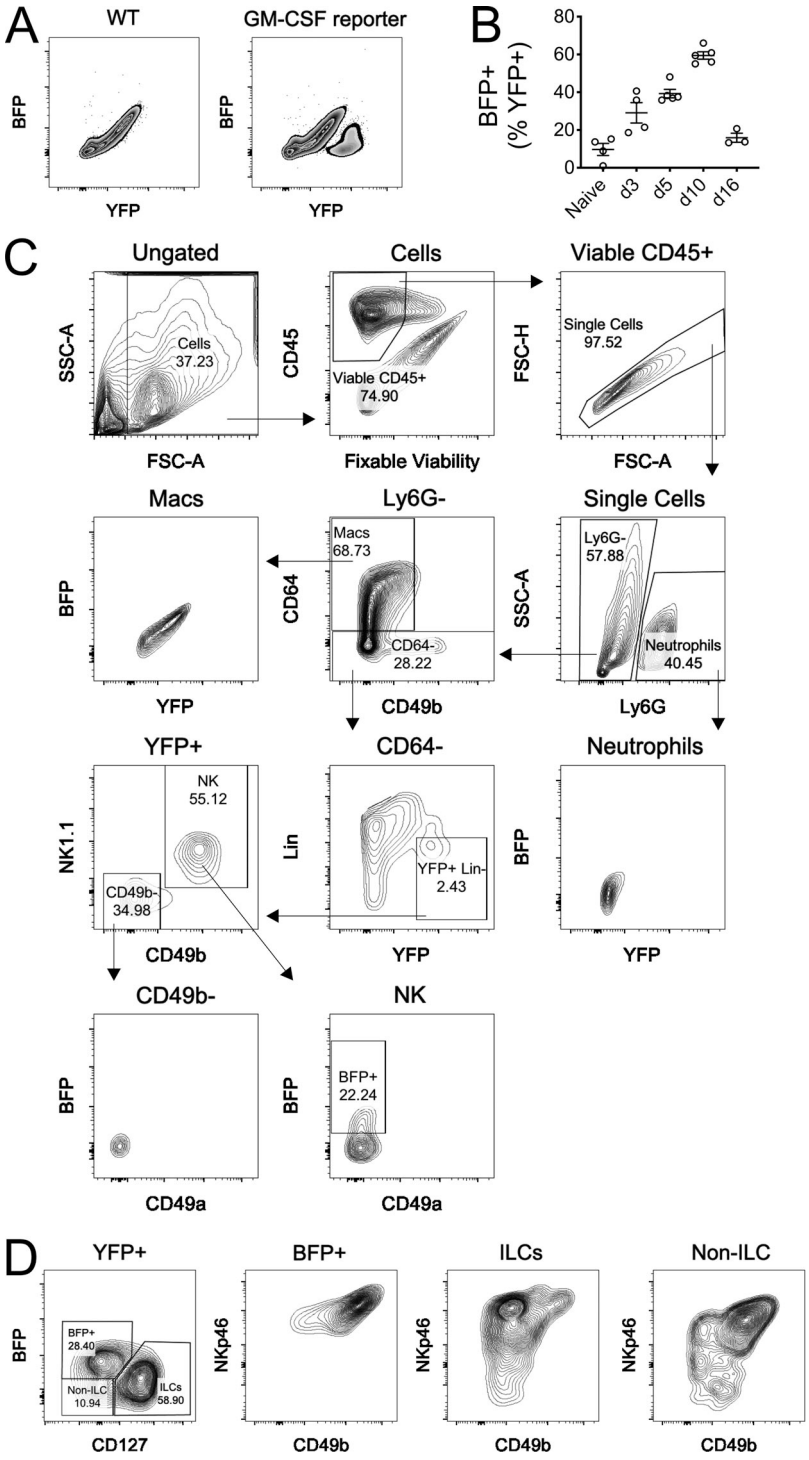

Figure 1. **NK cells produce GM-CSF in STIA. (A)** Representative FACS plots showing GM-CSF–producing cells (BFP^+YFP^+) in the inflamed joints of WT or Gr/fr mice with STIA. **(B)** Proportion of GM-CSF-producing (BFP^+) cells among GM-CSF producers (total YFP^+) cells in the STIA inflamed joints of Gr/fr mice across various time points of arthritis. Vertical bars, mean ± SEM, n = 3–5 mice. **(C)** Representative FACS plots showing gating strategies used to identify GM-CSF–producing cells (BFP^+YFP^+) among joint-infiltrating immune cells in the Gr/fr mice with STIA. Data shown for A–C are representative of two independent experiments. **(D)** Representative FACS plots showing segregation of GM-CSF–producing cells (BFP^+YFP^+) and other cells with a history of producing GM-CSF (BFP^- YFP^+) in Gr/fr mice with STIA. FSC-A, forward scatter area; SSC-A, side scatter area.

day 10 and resolves spontaneously by day 16 (Fig. 1 B). The majority of exudate cells in the STIA joints were $Ly6G^+$ neutrophils and $CD64^+$ macrophages (Fig. 1 C). Neutrophils and macrophages were highly autofluorescent, but were BFP^- YFP^- (Fig. 1 C). In contrast, YFP^+ cells were identified in the non-myeloid ($Ly6G^-$ $CD64^-$), Lin^- (TCRβ, CD3ε, CD19) fraction, and BFP^+ cells were evident in the $CD49b^+$ $NK1.1^+$ NK cell gate (Fig. 1 C). As shown in Fig. 1 D, almost all BFP^+ cells were mature NK cells ($CD127^-$ $NKp46^+$ $CD49b^+$), while other cells with a history of producing GM-CSF (BFP^- YFP^+) were primarily other ILC subsets ($CD127^+$ $NKp46^+$ $CD49b^-$). BFP^- YFP^+ $CD127^-$ non-ILCs comprised the remaining fraction of $CD49b^+$ $NKp46^+$ NK cells (Fig. 1 D). Of note, BFP^+ cells were mainly found in the viable $CD45^+$ gate, indicating nonhematopoietic cells are minimal contributors to GM-CSF production in STIA (Fig. S1 D). These results demonstrate that NK cells are recruited to inflamed joints and produce GM-CSF during STIA.

To corroborate our findings from the mouse system, we analyzed synovial fluid (SF) cells from RA patients with high levels of anti-cyclic citrullinated peptide antibodies, and peripheral

blood cells from healthy donors as controls. As reported previously (Dalbeth and Callan, 2002; Yamin et al., 2019), SF-infiltrating NK cells were mainly immature CD56^{bright} cells, which is a potent cytokine-producing subset (Caligiuri, 2008), in contrast to the mostly mature CD56^{dim} cytotoxic subset found in the peripheral blood of healthy donors (Fig. S2, A to B). Because CD4$^+$ T cells are known to be GM-CSF producers (Reynolds et al., 2016), we also examined the composition of the GM-CSF–, or GM-CSF/IFN-γ–expressing T and NK cell compartment from SF samples from three RA patients (Fig. S2 C). As expected, CD4 T cells from RA patients produced GM-CSF, or GM-CSF and IFN-γ, at higher frequencies than other T cells (such as CD8 T cells), as shown by intracellular staining (Fig. S2, C–E). However, synovial NK cells also constituted a significant proportion of GM-CSF–producing cells (Fig. S2 D). These data confirm that CD4 Th cells are a major source of GM-CSF, but reveal that NK cells can also contribute to the production of GM-CSF in RA.

NK cells contribute to the maintenance of autoantibody-induced arthritis

To determine if NK cells directly contribute to the pathogenesis of STIA, we examined disease development in *Mcl1*$^{fl/fl}$:Ncr1-Cre NK-deficient mice (Sathe et al., 2014) and anti-NK1.1–treated NK depleted mice. The onset of STIA was comparable in NK-deficient mice relative to NK-sufficient mice, but there was consistently reduced disease severity at later time points (Fig. 2, A and B). Flow-cytometric analysis confirmed reduction in the numbers of NK cells, neutrophils, and macrophages in the joints of both *Mcl1*$^{fl/fl}$:Ncr1-Cre and anti-NK1.1–treated WT mice (Fig. 2, A and B), relative to control mice.

To ascertain whether cytokine-production by NK cells is functionally important in STIA, we induced STIA in CD45$^{-/-}$ mice. CD45$^{-/-}$ mice have an expanded NK compartment and intact cytolytic capacity, but are unable to produce cytokines following stimulation of Fc receptors, due to impaired signal transduction (Hesslein et al., 2006; Huntington et al., 2005). Similar to NK-deficient mice, CD45$^{-/-}$ mice had equivalent disease onset, but lower arthritis severity at later time points (Fig. 2 C). CD45$^{-/-}$ mice had an intact synovial NK cell population, but still developed less neutrophil and macrophage infiltration of inflamed joints (Fig. 2 C). These data suggest that the cytokine-producing function of NK cells, rather than NK cell cytotoxicity, promotes STIA.

Following our observation that NK cells produce GM-CSF during STIA (Fig. 1 C) and because NK cells are well-known producers of IFN-γ during inflammation, we compared STIA in GM-CSF$^{-/-}$ and IFN-γ$^{-/-}$ mice to determine the relative contributions of these inflammatory cytokines. GM-CSF$^{-/-}$ but not IFN-γ$^{-/-}$ mice had reduced arthritis severity (Fig. 2, D and E), highlighting a pathogenic role for GM-CSF rather than IFN-γ in promoting STIA. Neither GM-CSF nor IFN-γ deficiency affected the numbers of joint NK cells, but GM-CSF$^{-/-}$ mice had less joint-infiltrating neutrophils and macrophages (Fig. 2, D and E), paralleling reduced arthritis severity. Taken together, these results show that NK cells promote autoantibody-induced inflammatory arthritis through GM-CSF, rather than IFN-γ, production.

GM-CSF production by NK cells promotes the persistence of autoantibody-induced arthritis

To control GM-CSF expression in vivo, we generated *Csf2*$^{fl/fl}$ mice (Fig. 3 A). We then generated *Csf2*$^{fl/fl}$:Ncr1-Cre mice to delete GM-CSF production specifically in NK cells. We confirmed that GM-CSF, but not IFN-γ, production was specifically depleted in splenic NK cells of *Csf2*$^{fl/fl}$:Ncr1-Cre mice following in vitro stimulation with IL-15 and IL-18 (Fig. 3 B). Importantly, *Csf2*$^{fl/fl}$:Ncr1-Cre mice (Fig. 3 C) recapitulated the reduced STIA of NK- or GM-CSF–deficient mice (Fig. 2, A, B, and D), including reduced numbers of synovial neutrophils and macrophages, but not synovial NK cells (Fig. 3 C). Intracellular GM-CSF staining confirmed GM-CSF deletion in synovial NK cells from arthritic *Csf2*$^{fl/fl}$:Ncr1-Cre mice relative to *Csf2*$^{fl/fl}$ mice (Fig. 3 D). To determine the effect of NK cell–derived GM-CSF in another model of inflammatory arthritis, we examined CIA, which is also dependent on autoantibodies generated following immunization to type II collagen (Svensson et al., 1998). Again, we found no difference in the onset of CIA, but a reduction in the progression and severity of inflammatory arthritis in the *Csf2*$^{fl/fl}$:Ncr1-Cre mice (Fig. 3 E). These results demonstrate that NK cells contribute to the persistence of autoantibody-induced inflammatory arthritis via GM-CSF production.

IL-18 controls GM-CSF production by synovial NK cells

IL-18 can induce GM-CSF production by NK cells in vitro (Brady et al., 2010; Fig. 3 B), and IL-18 has been shown to be produced by synovial macrophages from RA, but not osteoarthritis, patients (Gracie et al., 1999). Joint lavage from WT STIA mice showed elevated IL-18 (Fig. 4 A). We therefore assessed the relevance of IL-18 to GM-CSF production by NK cells in STIA. IL-18$^{-/-}$ mice had reduced STIA (Fig. 4 B) and less synovium-infiltrating myeloid cells (Fig. 4 C). While the number of joint NK cells in IL-18$^{-/-}$ mice was comparable to WT mice (Fig. 4 C), intracellular GM-CSF staining confirmed a reduced frequency of GM-CSF–producing synovial NK cells (Fig. 4 D). Consistent with reduced GM-CSF production, levels of secreted GM-CSF and CCL17 were also lower in the joint lavages of IL-18$^{-/-}$ mice (Fig. 4 E). Taken together, these findings show that IL-18 augments GM-CSF production by synovial NK cells in STIA.

GM-CSF induces CIS to limit JAK2-STAT5 signaling in myeloid cells

Our understanding of how GM-CSF signaling is regulated remains incomplete (Becher et al., 2016; Wicks and Roberts, 2016). Many cytokines induce SOCS proteins to negatively regulate signaling via inhibition of STAT binding to the receptor complex, or proteasome-mediated degradation of signaling components (Morris et al., 2018). To explore mechanisms regulating GM-CSF signaling, we profiled GM-CSF–induced SOCS expression in purified mouse bone marrow (BM) neutrophils. GM-CSF induced *Cish* and *Socs3* mRNA within 2 h of GM-CSF treatment, but only *Cish* mRNA levels were sustained at later time points, and these were more prominent than *Socs3* mRNA (Fig. 5 A). In contrast, granulocyte-colony stimulating factor (G-CSF) modestly induced a transient up-regulation of *Socs3* mRNA in neutrophils (Fig. 5 A), consistent with SOCS3 being the inducible

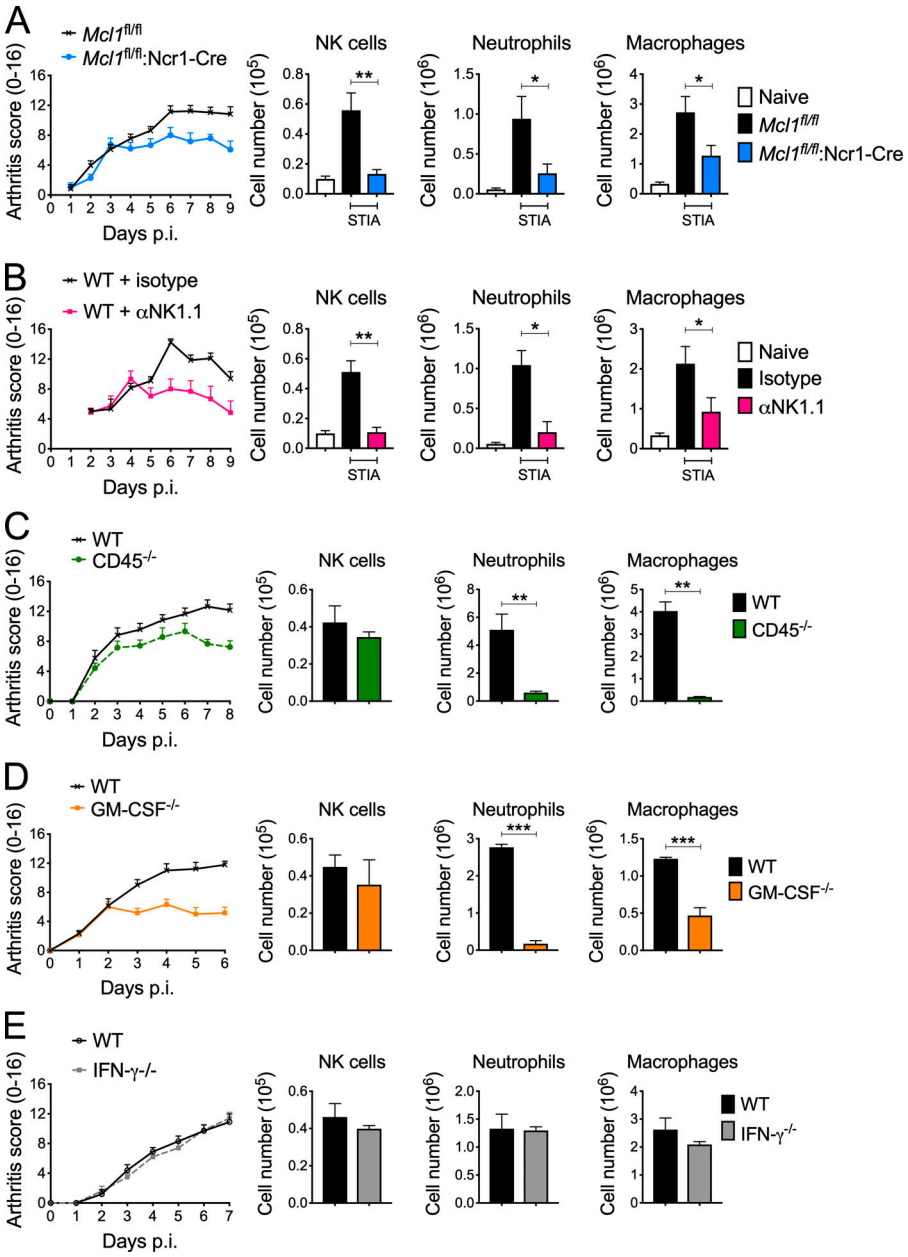

Figure 2. **NK cells are involved in the persistence of STIA. (A–E)** STIA was induced by K/BxN serum injection in (A) NK-deficient *Mcl1*$^{fl/fl}$:Ncr1-Cre mice or NK-sufficient *Mcl1*$^{fl/fl}$ mice (n = 18 mice pooled from three independent experiments, SEM), (B) NK-deficient (anti-NK1.1–treated) or NK-sufficient (isotype-treated; n = 12 mice pooled from two independent experiments, SEM), (C) WT or CD45$^{-/-}$ (intact population but functionally deficient NK cells (n = 6 mice from one experiment, SEM), (D) WT or GM-CSF$^{-/-}$ (n = 12 mice pooled from two independent experiments, SEM), and (E) WT or IFN-γ$^{-/-}$ (n = 6 mice from one experiment, SEM). Arthritis development was monitored daily, and FACS-based quantification of joint cell infiltrates (NK cells, neutrophils, and macrophages) was performed at the end of the experiment. p.i., post-injection. *, P < 0.05; **, P < 0.01; ***, P < 0.001.

negative regulator of G-CSF signaling (Croker et al., 2004). CIS induction and STAT5 phosphorylation following GM-CSF stimulation also occurred in human neutrophils and monocytes (Fig. S3 A).

Given consistent CIS induction following GM-CSF stimulation in GM-CSFR–expressing primary myeloid cells (Fig. 5 A and Fig. S3 A), we hypothesized that CIS acts as a molecular brake on GM-CSF signaling. We therefore examined GM-CSF–induced activation of the JAK-STAT pathway in CIS-deficient mice (Delconte et al., 2016; Palmer et al., 2015). Steady-state numbers of myeloid cells (neutrophils, monocytes, conventional dendritic cells, and macrophages) in BM, blood, spleen, and peritoneal cavity were comparable in CIS$^{-/-}$ mice compared with WT mice (Fig. S3 B). The normal myeloid compartment of CIS$^{-/-}$ mice is consistent with GM-CSF not playing a role in steady-state myelopoiesis (i.e., apart from the lung; Stanley et al., 1994). Freshly isolated WT or CIS$^{-/-}$ neutrophils lack JAK2-STAT5 activation (Fig. 5 B), consistent with negligible GM-CSF production in the steady-state (Wicks and Roberts, 2016). Following GM-CSF stimulation, CIS$^{-/-}$ neutrophils had similar phosphorylation kinetics for STAT5, p38 MAPK, SAPK/JNK, Erk1/2, and Akt1 relative to WT neutrophils at early time points (up to 1 h; Fig. 5 B). However, while the phosphorylation of STAT5 then declined in WT neutrophils, CIS$^{-/-}$ neutrophils had prolonged expression of STAT5 activation at later time points (2 h after stimulation; Fig. 5 B). Extended JAK2-STAT5 activation was also observed in GM-CSF–primed CIS$^{-/-}$ neutrophils after cytokine withdrawal (Fig. 5 C). In contrast, the kinetics of STAT3 and Akt dephosphorylation were similar between WT and CIS$^{-/-}$ neutrophils (Fig. 5 C). Consistent with extended JAK2-STAT5 activation in the absence of CIS, we also observed prolonged activation of p38 MAPK and SAPK/JNK (Fig. S3 C).

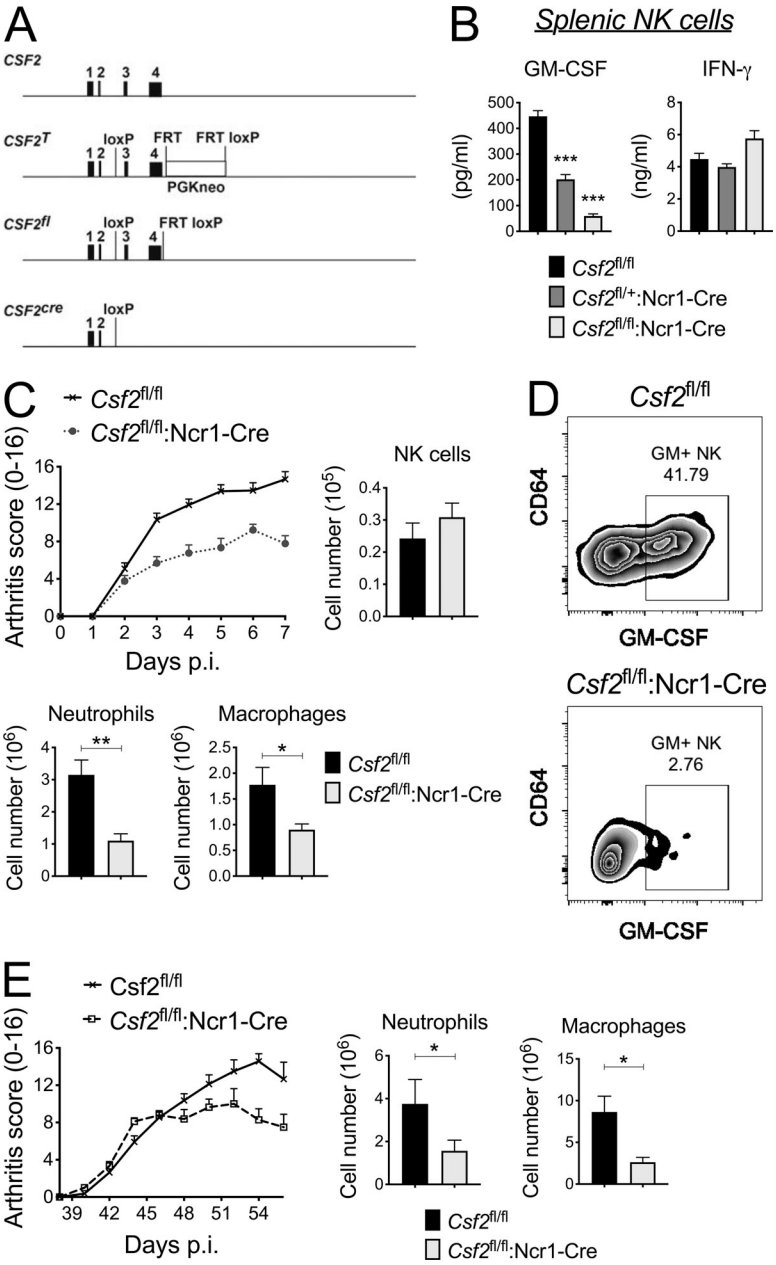

Figure 3. **GM-CSF deletion in NK cells alleviates STIA and CIA. (A)** Schematic representation of *Csf2*$^{fl/fl}$ mice with *loxP* sites flanking exon 3–4 for conditional deletion of *Csf2* (GM-CSF) upon crossing with mice carrying specific Cre recombinase under promoter of interest. **(B)** GM-CSF and IFN-γ analyzed by ELISA in culture supernatant of purified splenic NK cells from *Csf2*$^{fl/fl}$, *Csf2*$^{fl/+}$:Ncr1-Cre and *Csf2*$^{fl/fl}$:Ncr1-Cre mice following stimulation with IL-15 and IL-18 (n = 6 mice pooled from two independent experiments, SEM). **(C)** STIA development and FACS-based quantification of joint cell infiltrates in *Csf2*$^{fl/fl}$ and *Csf2*$^{fl/fl}$:Ncr1-Cre mice (n = 12 mice pooled from two independent experiments, SEM). **(D)** Representative intracellular GM-CSF staining of NK cells in the joints of *Csf2*$^{fl/fl}$ and *Csf2*$^{fl/fl}$:Ncr1-Cre mice upon STIA induction as in C. **(E)** Development of CIA and FACS-based quantification of joint cell infiltrates in *Csf2*$^{fl/fl}$ and *Csf2*$^{fl/fl}$:Ncr1-Cre (n = 18 mice from one experiment, SEM). *, P < 0.05; **, P < 0.01; ***, P < 0.001.

SOCS proteins negatively regulate cytokine signaling through direct inhibition, or proteasome-mediated degradation of signaling components (Morris et al., 2018). Basal expression of cell surface GM-CSFRβ was comparable in BM neutrophils from 50:50 WT:CIS$^{-/-}$ chimera mice (Fig. 5 D). However, following exposure to GM-CSF in vitro, CIS$^{-/-}$ neutrophils had higher cell surface GM-CSFRβ expression compared with WT cells. There was no such difference in G-CSF–stimulated cells (Fig. 5 D). In silico analysis using surface plasmon resonance of motifs in the ligand binding α chain of the GM-CSFR did not reveal obvious targets for CIS, but we identified a potential CIS binding site corresponding to the amino acid sequence around the pTyr 822 residue of mouse GM-CSFRβ, and the pTyr 882 residue of human GM-CSFRβ. The predicted binding affinity at this putative interaction site is ∼1 µM, which could potentially allow CIS to contribute to ubiquitination-mediated receptor turnover (Fig. 5 E). CIS may therefore act as a negative regulator of GM-CSF signaling in myeloid cells via proteasome-mediated degradation of GM-CSFRβ.

CIS-deficient neutrophils display extensive changes in response to GM-CSF

To examine the consequences of exaggerated GM-CSF signaling in the absence of CIS, we performed 75-bp single-ended RNA sequencing with simultaneous global proteomic validation on WT and CIS$^{-/-}$ neutrophils, purified directly from murine BM (unstimulated), or following culture with GM-CSF. Very few differentially expressed genes were observed in unstimulated CIS$^{-/-}$ neutrophils compared with WT (Fig. S4 A). Similarly, there was little difference in gene expression following GM-CSF stimulation for 4 h (Fig. S4 B), consistent with the delayed kinetics of CIS induction. However, CIS$^{-/-}$ neutrophils displayed

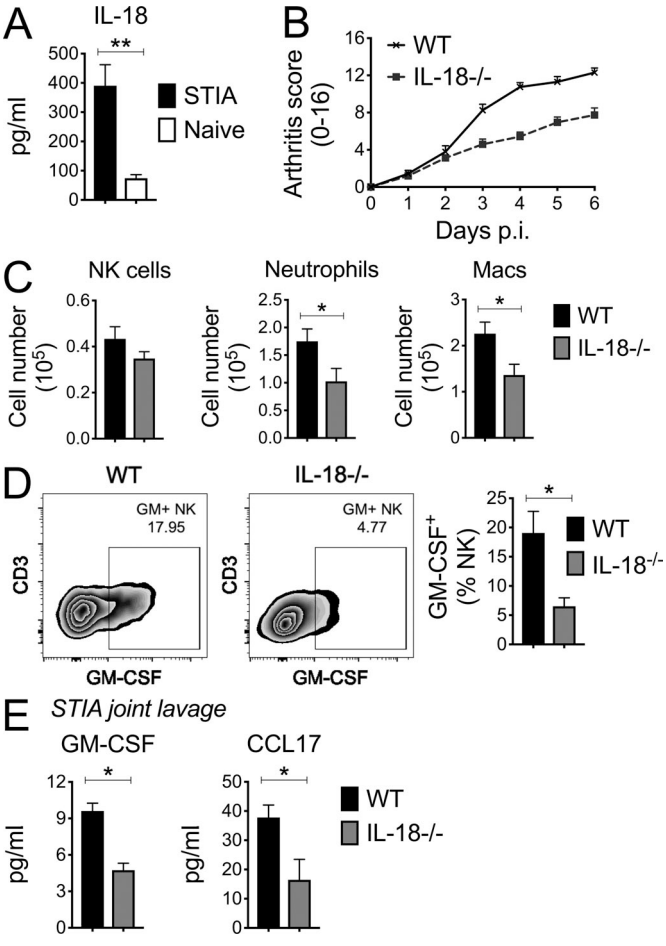

Figure 4. **IL-18 controls GM-CSF production by synovial NK cells.** STIA was induced by K/BxN serum injection in WT or IL-18$^{-/-}$ mice. **(A)** ELISA of arthritic (STIA) and naive SF from WT mice (n = 8 mice pooled from two independent experiments, SEM). **(B and C)** Arthritis development and (C) FACS-based quantification of joint cell infiltrates in WT or IL-18$^{-/-}$ mice (n = 18 mice pooled from three independent experiments, SEM). Macs, macrophages. **(D)** Intracellular GM-CSF staining of NK cells in the arthritic joints of WT or IL-18$^{-/-}$ mice as in B and C. **(E)** ELISA of arthritic SF from WT and IL-18$^{-/-}$ mice (n = 8 mice pooled from two independent experiments, SEM). *, P < 0.05; **, P < 0.01.

extensive transcriptional changes 24 h after GM-CSF stimulation (Fig. S4 C). The highest up-regulated transcripts included those for chemokines, such as *Cxcl3*, *Cxcl2*, *Ccrl2*, *Ccl4*, and *Pecam1*, and those associated with inflammatory effector functions, such as *Spp1*, *Edn1*, *Il1a*, *Ptgs2*, *Clec4n*, *Il1b*, *Plaur*, and *Il1f9* (Fig. 6 A). Global proteomic analysis elucidated additional mechanisms by which CIS deficiency might endow neutrophils with an enhanced pro-inflammatory phenotype in response to GM-CSF (Fig. 6 B). CIS-deficient neutrophils also demonstrated down-regulated protein expression, including matrix metalloprotease 8 (MMP8) and CYP4F3 (leukotriene B4/LTB4 omega-hydroxylase 2). Loss of MMP8 has been associated with exacerbation of arthritis due to its role in regulating neutrophil apoptosis (Cox et al., 2010; García et al., 2010). CYP4F3, also known as leukotriene B4/LTB4 omega-hydroxylase 2, also negatively regulates inflammation by catalyzing the inactivation of LTB4 (Bramwell et al., 2014, 2015; Chou et al., 2010; Christmas et al., 1999). Taken together, these findings highlight CIS as a negative regulator of GM-CSF–mediated neutrophil effector cell functions.

GM-CSF exerts various effects on myeloid cells, including promoting survival and priming an inflammatory phenotype (Croxford et al., 2015; Wicks and Roberts, 2016). To examine whether CIS$^{-/-}$ neutrophils exhibit a GM-CSF–dependent survival advantage, we examined survival-related proteins in WT and CIS$^{-/-}$ mice BM neutrophils following cytokine priming and withdrawal. Both WT and CIS$^{-/-}$ neutrophils had rapid induction of cleaved caspase-3 upon G-CSF withdrawal (Fig. S5 A). In contrast, GM-CSF withdrawal resulted in delayed induction of cleaved caspase-3 in CIS$^{-/-}$ relative to WT neutrophils (Fig. S5 A), consistent with enhanced bioactivity of GM-CSF on target cells. In keeping with published literature, GM-CSF selectively induced the pro-survival protein A1/Bfl-1 (Vier et al., 2016), and its level was sustained for a longer period in CIS$^{-/-}$ neutrophils upon GM-CSF withdrawal (Fig. S5 A). There was no difference in the expression of prosurvival Mcl-1 protein in WT and CIS$^{-/-}$ neutrophils, regardless of G-CSF or GM-CSF preconditioning (Fig. S5 A).

RNA sequencing (RNASeq) data also revealed an enhanced chemokine response in CIS$^{-/-}$ neutrophils (Fig. 6 A). CIS$^{-/-}$ neutrophils secreted higher levels of CXCL2 and CCL3 chemokines upon GM-CSF stimulation (Fig. S5 B). Moreover, CIS$^{-/-}$ neutrophils displayed enhanced cell surface CCRL2 expression following GM-CSF, but not G-CSF, stimulation (Fig. S5, C and D). These chemokine responses promote tissue inflammation (Chou et al., 2010; Del Prete et al., 2017; Jacobs et al., 2010). Thus, CIS deficiency confers extended GM-CSF signaling that endows neutrophils with a prolonged lifespan and exaggerated, proinflammatory chemokine responses. Collectively, these enhanced neutrophil responses to GM-CSF help explain the cellular basis for exacerbated tissue inflammation in the absence of CIS.

GM-CSF induces the differentiation of monocytes into CD11c^{+} macrophages (GM-Macs; Helft et al., 2015) and the production of CCL17 and CCL22 by monocytes (Achuthan et al., 2016; Croxford et al., 2015). Consistent with enhanced GM-CSF signaling, CIS-deficient monocytes underwent accelerated differentiation into GM-Macs in response to GM-CSF, relative to WT monocytes (Fig. S5 E). Moreover, CIS$^{-/-}$ monocytes produced higher levels of chemokines following GM-CSF stimulation (Fig. S5 F). Thus, prolonged GM-CSF signaling in the absence of CIS also resulted in exaggerated GM-CSF–driven responses in monocytes, which would also worsen GM-CSF–driven inflammation.

IL-3 and IL-5 also signal through the common β chain and can induce *Cish* expression in common myeloid progenitors and eosinophils, respectively (Burnham et al., 2013; Matsumoto et al., 1997; Yoshimura et al., 1995). Therefore, CIS deficiency should confer exaggerated cellular responses to these cytokines. Indeed, CIS$^{-/-}$ BM cells generated greater numbers of common myeloid progenitors in response to IL-3 (Fig. S5 G), and of eosinophils in response to IL-5 (Fig. S5 H).

Taken together, these data demonstrate that in the absence of CIS, GM-CSF signaling is unrestrained and leads to enhanced GM-CSF–dependent responses in myeloid cells, such as up-regulation of proinflammatory chemokines by neutrophils and

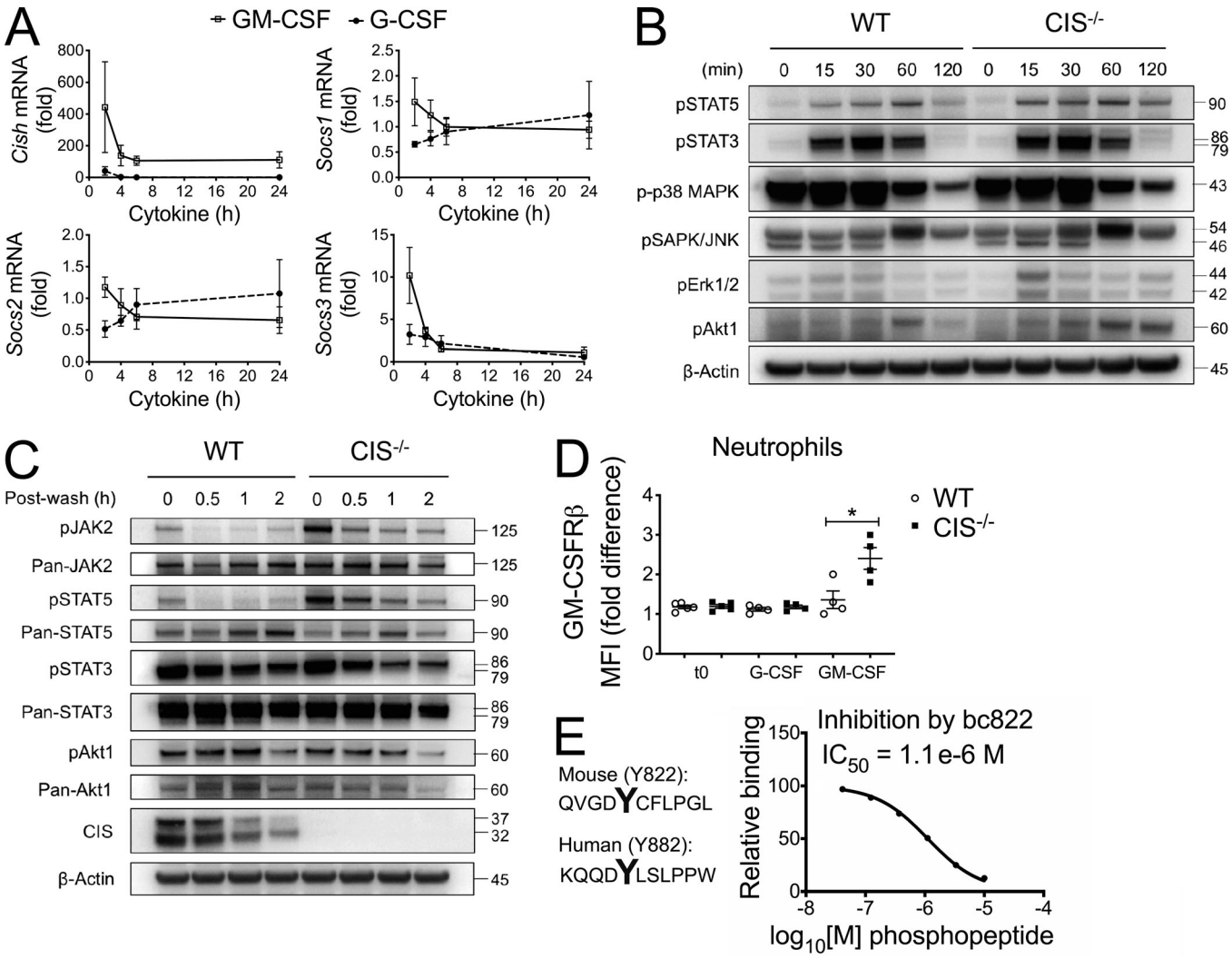

Figure 5. **GM-CSF induces CIS to limit JAK2-STAT5 signaling in myeloid cells. (A)** Expression of mRNA for SOCS proteins (*Cish*, *Socs1*, *Socs2*, and *Socs3*) by WT mouse BM neutrophils analyzed by real-time PCR, normalized to *Gapdh*, at indicated times after stimulation with G-CSF or GM-CSF (n = 4 mice pooled from two independent experiments, SEM). Data are expressed as fold induction relative to unstimulated neutrophils. **(B)** Immunoblot analysis of WT or CIS$^{-/-}$ BM neutrophils stimulated in vitro with 100 ng/ml GM-CSF for indicated times. **(C)** Immunoblot analysis of WT or CIS$^{-/-}$ BM neutrophils primed with GM-CSF for 3 h, then washed, and cultured in cytokine-free media at various times post-wash. MFI, mean fluorescence intensity. **(B and C)** One experiment representative of three independent experiments with similar results. **(D)** Flow-cytometric analysis of CD131 (GM-CSFRβ) surface expression on naive (t0) and G-CSF or GM-CSF–stimulated BM neutrophils from WT:CIS$^{-/-}$ (50:50) chimeric mice (n = 4 mice pooled from two independent experiments, SEM). Data are expressed as fold induction relative to unstimulated WT neutrophils. **(E)** Putative binding sites and affinity of CIS-SH2-BC to phosphopeptides corresponding to tyrosines in the mouse and human GM-CSFRβ cytoplasmic domain. Data are from two experiments. *, P < 0.05.

monocyte-derived macrophages, which may translate to intensified, GM-CSF–driven inflammation in vivo.

CIS$^{-/-}$ mice develop exacerbated GM-CSF–driven inflammation

Given these cellular and biochemical data, we directly investigated the effect of CIS deficiency in the STIA model. CIS$^{-/-}$ mice developed clinically exacerbated STIA compared with WT mice (Fig. 7 A), which was confirmed by in vivo imaging for myeloperoxidase activity (Fig. 7 B). Lavage of inflamed joints showed CIS$^{-/-}$ mice had comparable levels of GM-CSF and TNF, but higher levels of pro-inflammatory cytokines and chemokines, including IL-1β, LTβ4, CXCL2, CCL3, and CCL17 (Fig. 7 C). Of note, increased levels of these proinflammatory mediators in the arthritic joints of CIS$^{-/-}$ mice parallel the exaggerated chemokine responses of GM-CSF–exposed neutrophils seen on RNASeq (Fig. 6 A), and reduced expression of negative regulators of inflammation, as revealed by proteomics (Fig. 6 B).

Exaggerated arthritis in the CIS$^{-/-}$ mice during STIA may stem from dysregulated GM-CSF responses in neutrophils and/or inflammatory monocytes, because these myeloid cells predominate in the inflamed joints and express the GM-CSFR. However, Ly6C^{+} inflammatory monocytes are redundant in STIA because CCR2$^{-/-}$ mice (which lack these Ly6C^{+} inflammatory monocytes) can still develop fulminant STIA (Misharin et al., 2014). Thus, GM-CSF signaling, even in the absence of Ly6C^{+} inflammatory monocytes, can support arthritis. To determine whether GM-CSF signaling in neutrophils is indeed responsible in driving the persistence of STIA, we generated

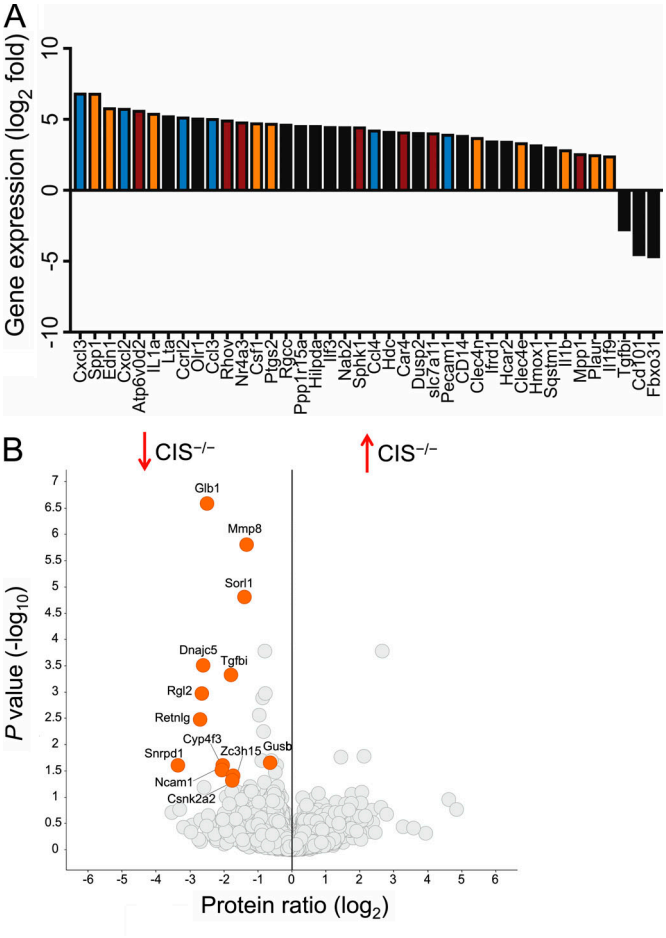

Figure 6. **CIS-deficient neutrophils display extensive transcriptional and proteomic changes in response to GM-CSF. (A)** Quantitative RNA transcript analysis (vertical axis, reads per kilobase of exon per million reads) of purified WT and CIS$^{-/-}$ BM neutrophils was performed by RNASeq following GM-CSF stimulation for 24 h. Selected genes that were differentially expressed in CIS$^{-/-}$ neutrophils are shown (n = 3 biological replicates). **(B)** Volcano plots representing the $\log_2$ protein ratios of differentially regulated proteins in CIS$^{-/-}$ relative to WT neutrophils following quantitative analysis. Proteins with a $-\log_{10}$ P > 1.3 and fold change >1 were deemed differentially expressed and are highlighted in orange (n = 3 biological replicates).

Csf2rb$^{fl/fl}$:Mrp8-Cre mice to specifically delete GM-CSFRβ in neutrophils (Fig. 7 D). Similar to GM-CSF$^{-/-}$, NK-deficient mice (anti-NK1.1-treated WT or *Mcl1*$^{fl/fl}$:Ncr1-Cre), and *Csf2*$^{fl/fl}$:Ncr1-Cre mice, *Csf2rb*$^{fl/fl}$:Mrp8-Cre mice had similar onset of arthritis but did not maintain arthritis at later time points (Fig. 7 E). This result suggests that GM-CSF signaling in neutrophils is specifically required for the persistence of STIA.

CIS deficiency also confers enhanced NK cell function, including cytokine production (Delconte et al., 2016). We examined if amplified production of GM-CSF by CIS$^{-/-}$ NK cells might provide another mechanism for enhanced joint inflammation. CIS$^{-/-}$ joint NK cells, however, produced comparable levels of GM-CSF as determined by intracellular FACS staining (Fig. 7 F), in keeping with comparable levels in the joint lavage (Fig. 7 C). However, consistent with NK cell and GM-CSF dependency, NK cell depletion or GM-CSF neutralization alleviated STIA in CIS$^{-/-}$ mice (Fig. 7 G).

Finally, we also examined the effect of CIS deficiency in the EAE model of central nervous system (CNS) inflammation. Consistent with previous reports that EAE is driven by encephalitogenic CD4 T cell–derived GM-CSF (Croxford et al., 2015; Komuczki et al., 2019), GM-CSF deletion by tamoxifen administration in *Csf2*$^{fl/fl}$:R26CreERT2 mice inhibited the progression of EAE (Fig. S5 I). Intracellular cytokine staining confirmed GM-CSF deletion but comparable IL-17A production in *Csf2*$^{fl/fl}$:R26CreERT2 mice relative to littermate control *Csf2*$^{fl/fl}$ mice (Fig. S5 J), consistent with a redundant role for IL-17A in driving EAE (Haak et al., 2009). Similar to the STIA model of inflammatory joint disease, CIS$^{-/-}$ mice developed exacerbated EAE (Fig. S5 K). This effect was not due to an up-regulation of cytokine production by CNS-infiltrating CD4 T cells (Fig. S5 L). Taken together, these results demonstrate a role for CIS as an inducible regulator of GM-CSFR signaling in myeloid cells that normally functions to limit tissue inflammation and immunopathology.

Discussion

In this study, we report two separate findings regarding GM-CSF regulation during autoantibody-mediated inflammatory arthritis. First, we show that GM-CSF is produced by synovial NK cells, and these cells contribute to the persistence of inflammatory arthritis. This is dependent on IL-18. Second, we reveal that GM-CSF signaling in joint- and CNS-infiltrating myeloid cells is negatively regulated by the inducible signaling suppressor CIS, validating CIS as an endogenous brake on GM-CSF–driven tissue inflammation.

The role of GM-CSF has been evaluated in the T cell–dependent SKG and EAE models of inflammatory arthritis and MS, respectively (Croxford et al., 2015; Hirota et al., 2018; Komuczki et al., 2019). Although a genetic association with RA has been described for the *CSF2* locus (Okada et al., 2012), it is unclear how GM-CSF contributes to the effector phase of tissue inflammation mediated by autoantibodies in RA. Using a T cell–independent, autoantibody-mediated arthritis model (STIA) in Gr/fr mice, we identified NK cells as the main producers of GM-CSF. NK cells are usually associated with production of IFN-γ (Souza-Fonseca-Guimaraes et al., 2012; Zitti and Bryceson, 2018), and IFN-γ–producing, CD56^{bright} NK cells are enriched in human RA synovium (Dalbeth and Callan, 2002; Yamin et al., 2019). Although these studies suggest IFN-γ as a key inflammatory mediator of arthritis, evidence for NK cell–derived IFN-γ as a direct contributor to inflammatory arthritis remains controversial in murine models (Lo et al., 2008; Söderström et al., 2010). Here, we show that the cytokine-producing function of NK cells, specifically GM-CSF rather that IFN-γ, is essential for sustaining autoantibody-driven joint inflammation in STIA. Genetic or pharmacologic depletion of NK cells, or abrogation of GM-CSF production by NK cells, did not prevent the early phase of inflammatory arthritis, but rather, it reduced the accumulation of an inflammatory cell infiltrate and the progression of inflammatory joint disease. GM-CSF–producing NK cells were also found in human inflammatory arthritis SF. GM-CSF production has been reported from both human and mouse NK cells (Cuturi et al., 1989; Ho et al.,

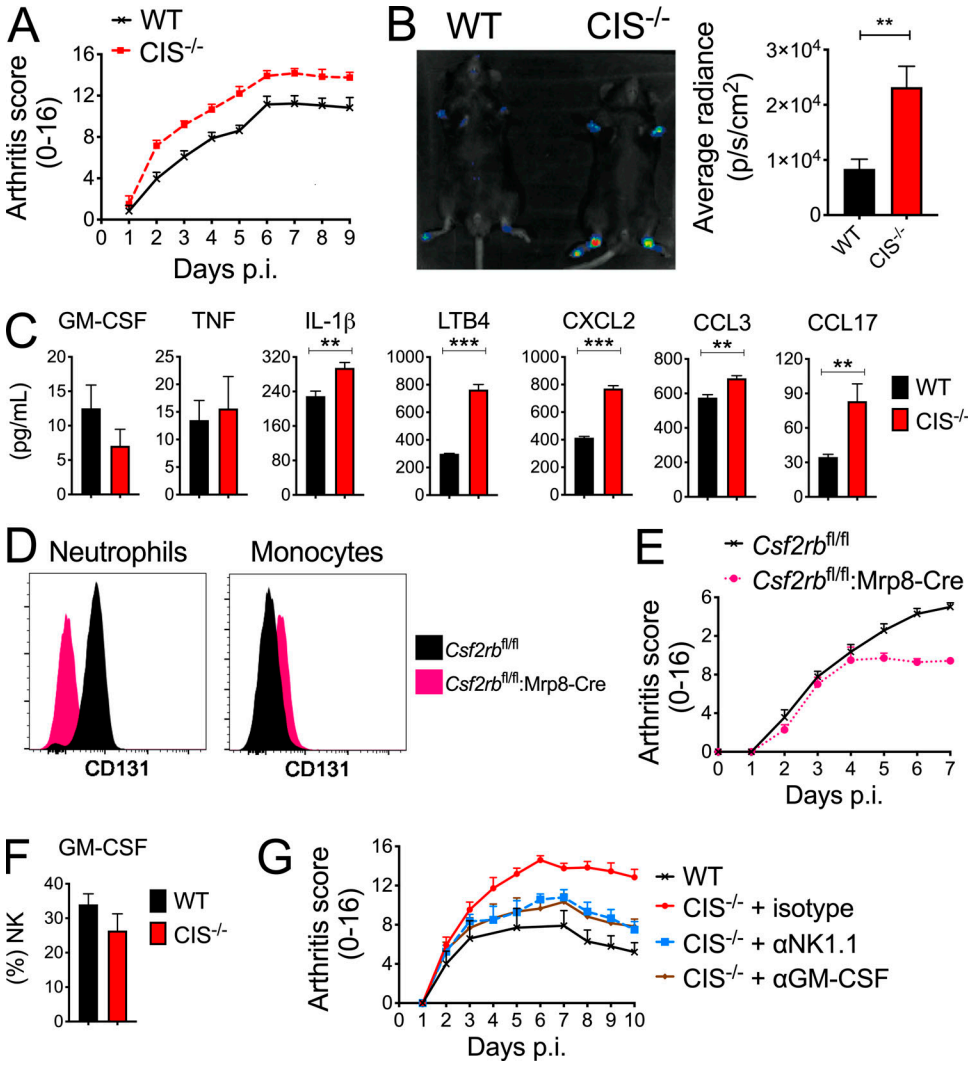

Figure 7. **CIS-deficient mice develop exacerbated STIA due to deregulated GM-CSF activation in neutrophils. (A)** Arthritis development of WT and CIS$^{-/-}$ mice (n = 12 mice pooled from two independent experiments, SEM). **(B)** Bioluminescence imaging of myeloperoxidase activity in the arthritic joints of WT and CIS$^{-/-}$ mice, quantified as average radiance (n = 8 mice pooled from two independent experiments, SEM). **(C)** Pro-inflammatory mediators (GM-CSF, TNF, IL-1β, LTB4, CXCL2, CCL3, and CCL17) analyzed by ELISA in SF of arthritic WT and CIS$^{-/-}$ mice (n = 8 mice pooled from two independent experiments, SEM). **(D)** Representative CD131 (GM-CSFRβ) expression in blood neutrophils and monocytes of *Csf2rb*$^{fl/fl}$ and *Csf2rb*$^{fl/fl}$:Mrp8-Cre mice (n = 6 mice from one experiment). **(E)** Arthritis development in *Csf2rb*$^{fl/fl}$ and *Csf2rb*$^{fl/fl}$:Mrp8-Cre mice (n = 6 mice from one experiment, SEM). **(F)** Intracellular GM-CSF staining of NK cells in the joints of WT and CIS$^{-/-}$ mice during STIA (n = 8 mice pooled from two independent experiments, SEM). **(G)** Arthritis development in WT and CIS$^{-/-}$ mice (treated with isotype, anti-NK1.1 or anti-GM-CSF mAbs; n = 12 mice pooled from two independent experiments, SEM). **, P < 0.01; ***, P < 0.001.

2002), but there is little information about the functional importance of NK cell–derived GM-CSF in a pathological context. Our results support the notion that GM-CSF–producing NK cells are an important component of an inflammatory cellular cascade that maintains antibody-mediated inflammatory arthritis.

It has been well substantiated that the cytokines TNF and IL-1, the alternative complement pathway, and innate immune cells such as neutrophils, monocytes, and macrophages are key players in the effector phase of STIA (Chou et al., 2010; Ji et al., 2002a, b; Misharin et al., 2014; Sadik et al., 2012; Wipke and Allen, 2001; Wipke et al., 2004). Human RA fibroblast-like synoviocytes can also produce GM-CSF in response to IL-1 and TNF (Alvaro-Gracia et al., 1991). However, using the Gr/fr system, we found that the majority of GM-CSF–producing cells during STIA are leukocytes and, more specifically, NK cells. Thus, while nonleukocytes (e.g., stromal cells and fibroblast-like synoviocytes) can produce GM-CSF, NK cell production seems more important in maintaining autoantibody-mediated arthritis. Furthermore, we found that the IL-1 family member IL-18 activates synovial NK cells to produce GM-CSF during STIA. RA synovial macrophages are known sources of IL-18, and exogenous IL-18 can promote the secretion of GM-CSF (along with nitric oxide, TNF, and IFN-γ) in synovial cell cultures (Gracie et al., 1999). Unlike IL-1–deficient mice, which cannot initiate STIA (Ji et al., 2002b), IL-18–deficient mice developed inflammatory arthritis, but this did not progress. This phenotype resembles that seen in GM-CSF– and NK-deficient mice. Thus, while IL-1 directly triggers the onset

of arthritis, IL-18 acts indirectly in STIA, by activating NK cells to secrete GM-CSF.

IL-18 has been linked to NK activation in antiviral responses (Madera and Sun, 2015; Mantovani et al., 2019). It has also been implicated in autoimmune inflammation, through adjuvant activity on T cells (Gracie et al., 1999; Lalor et al., 2011). It is tempting to speculate that immune complexes could be implicated in the production or release of IL-18. Alternatively, damage-associated molecular patterns released by stressed cells in the inflamed joint during STIA could in turn activate TLR signaling and IL-18–activating inflammasomes in synovial macrophages. Both IL-1β and IL-18 can be induced by TLR4 or TLR7 ligands, but IL-18 production is sustained after activation, while IL-1β up-regulation is transient (Zhu and Kanneganti, 2017). Potentially relevant ligands for TLR4 in arthritis include aberrant extracellular high mobility group box chromosomal protein 1 (HMGB1; Ostberg et al., 2010), citrullinated fibrinogen (Sokolove et al., 2011), and alarmins S100A8 and S100A9 (van Lent et al., 2008; van Lent et al., 2010). TLR7 ligands in RA SF have also been described such as single strand RNA, microRNA let-7b (miR-let-7b), or miR-let-7b–containing exosomes (Chamberlain et al., 2013; Kim et al., 2016). Similar to the reduced arthritis in IL-18–, NK cell–, and GM-CSF–deficient mice shown in this study, TLR-deficient mice ($TLR4^{-/-}$ and $TLR7^{-/-}$) can develop STIA, but with reduced severity (Choe et al., 2003; Duffau et al., 2015). Thus, we propose an immune cascade in which NK-derived GM-CSF contributes to the persistence of autoantibody-driven arthritis. However, we do not exclude contributions from GM-CSF–producing T cells, other ILC subsets, and nonlymphoid stromal cells to the various stages of acute and chronic inflammation in RA (Al-Mossawi et al., 2017; Hirota et al., 2018; Reynolds et al., 2016). Rather, we suggest GM-CSF–producing joint NK cells may play a key role in maintaining tissue inflammation, in addition to GM-CSF from other sources, produced at other times.

GM-CSF drives pathogenic inflammation in autoimmune disorders such as RA and MS, and its signaling therefore needs to be terminated after activation. Various SOCS family members have been suggested to be induced by and therefore control GM-CSF signaling (Bunda et al., 2013; Esashi et al., 2008; Jackson et al., 2004). Here, we have provided physiological evidence that CIS is a bona fide inhibitor of GM-CSF signaling, in a classic negative feedback manner. In agreement with earlier reports (Matsumoto et al., 1997; Yoshimura et al., 1995), CIS deletion resulted in the prolonged activity of JAK2-STAT5–dependent pathways, with a corresponding increase in GM-CSF–driven effects on neutrophil survival, macrophage differentiation, and chemokine production. Our in silico analysis further identified cytoplasmic tyrosine motifs in the GM-CSFRβ subunit that interact with CIS, which may allow CIS to induce receptor turnover through ubiquitination and proteasome-mediated degradation. Consistent with this prediction, we found elevated GM-CSFRβ expression in CIS-deficient neutrophils following GM-CSF stimulation. CIS deficiency also enhanced the biological effects from IL-3 and IL-5, the receptors for which share the βc chain. These findings strongly suggest that CIS targets the βc chain in this cytokine receptor family for proteasome-mediated turnover.

In keeping with the relative absence of circulating GM-CSF in healthy mice, CIS-deficient mice show no basal pathology or alteration in myeloid cell frequencies in hematopoietic compartments (Stanley et al., 1994), but developed exacerbated GM-CSF–dependent arthritis. GM-CSF–dependent tissue pathology may be mediated by discrete GM-CSF–responding myeloid cell types (Becher et al., 2016), such as $Ly6C^{+}$ inflammatory monocytes in the EAE model (Croxford et al., 2015) and eosinophils in the chronic colitis model (Griseri et al., 2015). Here, we confirm that neutrophils are key GM-CSF responders in the STIA setting, because specific deletion of GM-CSFRβ in neutrophils alleviated arthritis. Thus, the exacerbation of arthritis in CIS-deficient mice likely stems from the prolonged activity of JAK2-STAT5–dependent pathways and phenotypic changes in neutrophils following GM-CSF exposure in the inflamed joint microenvironment. Transcriptomic and secreted protein analyses of GM-CSF–primed CIS-deficient neutrophils revealed marked up-regulation of pro-inflammatory chemokines associated with arthritis, including CXCL2 and CCL3 (Chou et al., 2010; Jacobs et al., 2010). Additionally, proteomic analysis of GM-CSF–primed CIS-deficient neutrophils revealed down-regulation of key enzymatic brakes of inflammation, such as MMP8 and CYP4F3, relative to WT neutrophils. Importantly, MMP8 has been shown to control neutrophil apoptosis and resolution of arthritis (Cox et al., 2010; García et al., 2010), while CYP4F3 catalyzes the inactivation of pro-inflammatory LTB4 (Bramwell et al., 2014, 2015; Chou et al., 2010; Christmas et al., 1999). Reductions in these anti-inflammatory pathways in GM-CSF–primed CIS-deficient neutrophils are likely to have contributed to the exacerbation of STIA in CIS-deficient mice because joint LTB4 levels were elevated. Finally, we confirmed a role for CIS in inhibiting the pathogenic function of GM-CSF in EAE. CIS-deficient mice developed exacerbated EAE, but this was not due to alterations in GM-CSF or IL-17 production by CNS infiltrating CD4 T cells.

These data raise the possibility of several novel therapeutic strategies for RA, along with the anti–GM-CSF therapies that are already underway in clinical trials. First, modulating the function of NK cells through their activating and/or inhibitory receptors may impact on persistent tissue inflammation. Of note, activation of NK cells by blocking the inhibitory CD94/NKG2A receptor was shown to promote killing of pathogenic T follicular helper and Th17 cells and alleviated autoimmune responses in the CIA model (Leavenworth et al., 2011). Second, IL-18 inhibition may be a therapeutic possibility in RA. Such a rationale is supported by our data showing a role for IL-18 in promoting the GM-CSF–producing function of NK cells during inflammatory arthritis. Earlier evidence showed the ability of IL-18 to prime CIA (Gracie et al., 1999) and conversely, the alleviation of CIA following treatment with anti–IL-18 antibodies, or using its endogenous inhibitor IL-18–binding protein (Plater-Zyberk et al., 2001). Finally, CIS mimetics could be designed to raise intracellular stores of CIS in inflammatory cells and thereby suppress GM-CSF–driven inflammation. Given our findings on the role of CIS in regulating other cytokines that signal through the βc chain, CIS mimetics may also limit the detrimental effects of IL-3 in sepsis (Weber et al., 2015) or of IL-5 in allergic inflammation (Corren, 2011).

Our findings may also have implications for CIS inhibitors to increase JAK/STAT signaling in NK cells and CD8 T cells and thereby enhance antitumor cytotoxicity (Delconte et al., 2016; Palmer et al., 2015) and/or antitumor DC priming (Miah et al., 2012). Inhibition of CIS in this context could potentially skew tumor-resident myeloid/dendritic cell development and differentiation, which may impact on tumor antigen presentation and myeloid-derived suppressor cell differentiation. While such effects could be beneficial for treatment of the tumor, our findings suggest a note of caution with regard to possible exacerbation of any underlying autoantibody-mediated inflammatory disease.

In conclusion, we provide evidence that NK cells amplify joint inflammation in autoantibody-induced inflammatory arthritis by producing GM-CSF and that CIS is a physiological inhibitor of GM-CSF signaling, acting to restrain the inflammatory properties of myeloid cells. These data significantly extend our appreciation of regulatory networks between IL-18, GM-CSF, and NK cells, and suggest an underappreciated role for recruited NK cells in driving sterile inflammatory diseases.

Materials and methods

Mice

The following mouse strains were used: C57BL/6J, Ncr1-Cre (Narni-Mancinelli et al., 2011), CD45$^{-/-}$ (Huntington et al., 2005), *Mcl1*$^{fl/fl}$:Ncr1-Cre (Sathe et al., 2014), GM-CSF$^{-/-}$ (Stanley et al., 1994), IFN-$\gamma^{-/-}$ (Dalton et al., 1993), IL-18$^{-/-}$ (Takeda et al., 1998), CIS$^{-/-}$ (Palmer et al., 2015), *Csf2rb*$^{fl/fl}$ (Croxford et al., 2015), and Mrp8-Cre (Passegué et al., 2004). *Csf2*$^{fl/fl}$:Rosa26CreERT2, *Csf2*$^{fl/fl}$:Ncr1-Cre and *Csf2rb*$^{fl/fl}$:Mrp8-Cre mice were generated by crossing the strains described above. Gr/fr mice were generated by B. Ciric. All genetically modified mouse strains in this study were on the C57BL/6J background, bred and maintained at The Walter and Eliza Hall Institute. Both male and female mice at 8–12 wk of age were used for all experiments. Where appropriate and indicated, littermate controls were used. No biological replicate was excluded based on preestablished criteria. Cohort sizes are described in each figure legend, with levels of statistical significance. All experiments were approved by the Animal Ethics Committee of The Walter and Eliza Hall Institute.

Generation of Gr/fr mice

Gr/fr mice were generated by targeted integration, resulting in replacement of the WT GM-CSF gene (*Csf2*) with vector. The IRES-iCre-2A-BFP-SV40pA cassette was placed 25 bp after the STOP codon in exon 4 in the 3′ untranslated region of *Csf2*. The flippase recombinase target (FRT)–flanked Neo cassette (FRT-Neo-FRT) was placed 330 bp upstream of exon 4 in an intronic sequence and was later excised through breeding with flippase (FLP) transgenic mice. The short homology arm (SA) extends 2.1 kb 5′ to the Neo cassette and the long homology arm (LA) 6.2 kb 3′ to the IRES-iCre-2A-BFP-SV40pA cassette. Length in bps were as follows: SA, 2,085; Neo, 1,561; MA [middle homology arm], 466; IRES-iCre-2A-BFP, 2,686; and LA, 6,620. The transgenic construct has been designed to provide normal expression of GM-CSF, driven by natural control elements of *Csf2*. GM-CSF triggers the expression of iCre and BFP; given that BFP is downstream of iCre, all BFP^{+} cells should also be iCre^{+}. These mice were then crossed Rosa26eYFP to enable lineage tracing via iCre-mediated YFP expression.

Generation of GM-CSF flox mice

To generate *Csf2*$^{fl/fl}$ mice, a targeting vector was constructed at the Gene Recombineering Facility (Monash University, Melbourne, Australia), in which an FRT-PGK-neo-FRT-loxP cassette was inserted downstream of exon 4, along with a loxP site in intron 2. The vector was electroporated into C57BL/6J embryonic stem cells, and chimeric mice were generated from two independent embryonic stem cell clones bearing the correctly targeted locus. Heterozygous offspring were generated on a C57BL/6J background, the PGK-neo sequence was removed by intercrossing with transgenic mice ubiquitously expressing FLP recombinase (Farley et al., 2000), and homozygous *Csf2*$^{fl/fl}$ mice were produced by subsequent intercrosses. Genotyping was performed using the primers 5′-CACTTGGAACTGGGAACCTC-3′, 5′-TTGATTTCACCTCCCTTTGG-3′, and 5′-CCGTAGACCCTG CTGCAATA-3′, which generate PCR DNA fragment sizes of 269 bp, 349 bp, and 193 bp for WT, targeted (PGK-neo deleted), and post-cre recombined loci, respectively.

Human samples and primary cells

SF samples from RA patients of the Rheumatology Unit (Royal Melbourne Hospital, Melbourne, Australia) were obtained at the time of arthrocentesis (knee joints), and cellular fractions were analyzed by flow cytometry. RA patients met the American College of Rheumatology 2010 classification criteria and were seropositive for rheumatoid factor and anti-citrullinated peptide antibody. Samples from peripheral blood were taken from healthy donors through the Volunteer Blood Donor Registry. All samples used in this study were obtained under the approval of the institutional review boards of The Walter and Eliza Hall Institute and the Royal Melbourne Hospital. Written informed consent was obtained from all participants.

STIA and antibody treatment

Pooled serum from 8–12-wk-old arthritic K/BxN mice (Korganow et al., 1999; Monach et al., 2008) was transferred into recipient mice (100 µl) i.p. on day 0. Clinical assessment for each paw used the following scoring system: 0, no edema/erythema; 1, inflamed digits; 2, mild edema/erythema over one surface of paw; 3, edema/erythema involving the entirety of paw; and 4, edema/erythema involving the entirety of paw and joint ankylosis. Scores were added for all four paws for a composite score. Each experiment was performed two to five times to confirm reproducibility. Whenever possible, scoring was performed in a blinded manner. Mice were injected i.p. with anti-NK1.1 (clone PK136, 200 µg/injection) to deplete NK cells or anti–GM-CSF (clone MP1-22E9, 200 µg/injection) to neutralize GM-CSF. Antibody injections were given every 2 d starting on day 1, day 0 being the day of K/BxN serum injection.

CIA

CIA was induced by immunizing mice subcutaneously with type II chicken collagen emulsified in CFA on days 0 and 14, as

previously described (Inglis et al., 2008). Clinical assessment for each paw used the following scoring system: 0, no edema/erythema; 1, inflamed digits; 2, mild edema/erythema over one surface of paw; 3, edema/erythema involving the entirety of paw; and 4, edema/erythema involving the entirety of paw and joint ankylosis. Scores were added for all four paws to generate a composite score.

In vivo bioluminescence imaging of myeloperoxidase activity

On specified days, mice were injected i.p. with luminol (200 mg/kg) and anaesthetized (isoflurane inhalation) before bioluminescence imaging on an in vivo imaging systems spectrum instrument (Caliper; exposure time 180 s; binning 4, field of view 12.5 cm). Regions of interest were manually selected over front and rear paws using Living Image Software, and identical regions of interest were used for time-course analysis. C57BL/6J naive mice injected with luminol were used to control for background luminescence (~400 average radiance).

Induction of EAE and in vivo manipulation

Mice were immunized intradermally at the base of the tail with 200 µg $MOG_{35–55}$ (Mimotopes) in CFA (BD), and 200 ng pertussis toxin (Sapphire Bioscience) in PBS was administered intraperitoneally on day 0 and day 2, as described previously (Codarri et al., 2011). Clinical disease was monitored blinded to group, as follows: 0, no detectable signs of EAE; 1, distal limp tail; 2, complete limp tail; 1.5, limp tail and hind limb weakness; 2, unilateral partial hind limb paralysis; 2.5, bilateral partial hind limb paralysis; 3, complete bilateral hind limb paralysis; and 4, complete hind limb paralysis and unilateral forelimb paralysis. To ablate GM-CSF–producing cells in $Csf2^{fl/fl}$:Rosa26CreERT2 mice, tamoxifen was administered by oral gavage after onset in experimental $Csf2^{fl/fl}$:Rosa26CreERT2 mice and littermate $Csf2^{fl/fl}$ control animals.

Synovial joint lavage and immunophenotyping of cells from the joints and CNS

Skin from the ankles and feet was removed, and inflamed soft tissues 3 mm above the heel were dissected away from the tibia and collected, along with arthritic joints. Digits were disarticulated without breaking bones to avoid contamination with BM cells, soft tissues were cut into small pieces, and the tibiotalar joint was opened posteriorly to expose the synovial lining. To collect synovial/joint lavage, disarticulated paws (all four per mouse) were incubated in 1 ml cold sterile PBS with agitation for 30 min at 4°C; cell-free supernatant was collected for ELISA. Paw tissue was incubated in digestion buffer (2 mg/ml Collagenase IV, 1 mg/ml Dispase, and 0.5 mg/ml DNase I in PBS) for 30 min at 37°C, with agitation. For the EAE model, the brain and spinal cord were digested with 2 mg/ml Collagenase IV, 1 mg/ml Dispase, and 0.5 mg/ml DNase I in PBS for 30 min at 37°C with agitation, followed by myelin removal using a continuous 28% Percoll PLUS (GE) gradient for 30 min at 15,000 *g* at 4°C. Cells released during digestion were filtered through 70-µm nylon mesh, erythrocytes were lysed, and cells were stained with viability dyes, incubated with FcBlock, and stained with fluorochrome-conjugated antibodies (see Table S1 for antibodies, clones, fluorochromes, and manufacturers). Quantification of total cell numbers by flow cytometry was done using fluorescent beads (Beckman Coulter). For intracellular staining of GM-CSF ex vivo, joint cells were processed as described above, restimulated with Cell Stimulation Cocktail Plus Protein Transport Inhibitor for 4 h, then stained intracellularly with BD Cytofix/Cytoperm and Perm/Wash solutions. Data were acquired on a BD LSR Fortessa flow cytometer. Compensation and analysis of the flow cytometry data were performed using FlowJo software (Tree Star). "Fluorescence minus one" controls were used when necessary to set gates.

Cell isolation for in vitro stimulation

For quantitative real-time PCR, immunoblotting, and in vitro functional assays of myeloid cells (i.e., differentiation, survival, or chemokine secretion), neutrophils were purified from BM of C57BL/6J or $CIS^{-/-}$ mice by stepwise immunolabeling with biotinylated anti-Ly6G (Biolegend), anti-biotin microbeads, and positive selection with LS columns (Miltenyi Biotec). Subsequently, BM monocytes were isolated by stepwise immunolabeling with biotinylated anti-CD115 (Biolegend), anti-biotin microbeads, and positive selection with LS columns (Miltenyi Biotec). Cells of at least 95% purity were used for stimulation with recombinant G-CSF or recombinant GM-CSF (100 ng/ml) for indicated times.

NK cells from mouse spleen homogenates were enriched with an NK cell isolation kit (Miltenyi Biotec) and sorted (PI^- $CD3^-$ $CD19^-$ $TCR\beta^-$ $F4/80^-$ $NK1.1^+$ $NKp46^+$ $CD49b^+$ $CD49a^-$) on an ARIA Fusion cell sorter (BD Biosciences) to achieve a final purity of 99–100%. NK cells were cultured at 37°C in RPMI 1640 medium containing 10% FCS for 48 h. To assess cytokine production, NK cells were stimulated with 10 ng/ml of rIL-15, 50 ng/ml of rIL-18, and 50 pg/ml of rIL-12. At the endpoint, supernatant was recovered and IFN-γ and GM-CSF levels were measured by ELISA.

RNA isolation and quantitative real-time PCR

Total RNA was extracted from cells using an ISOLATE II RNA Mini Kit (Bioline), digested with RNase-free DNase I (Bioline), and reverse-transcribed into complementary DNA using SuperScript III reverse transcription (Invitrogen) and oligo(dT) primers (Promega). Quantitative real-time PCR was performed using Fast SYBR Green Master Mix (Thermo Fisher Scientific) on a ViiA 7 PCR System (Thermo Fisher Scientific). Primers for the genes assessed are shown in Table S1.

Immunoblotting

For immunoblotting, neutrophils from the BM were isolated by positive-selection immunomagnetic enrichment using anti-Ly6G biotin, followed by anti-biotin microbeads and an LS column (Miltenyi Biotec). Monocytes were then isolated using anti-CD115 biotin, anti-biotin microbeads, and LS columns. The purity of enriched cells was consistently >95%. Cells were stimulated in vitro with recombinant G-CSF (100 ng/ml) or recombinant GM-CSF (100 ng/ml) for indicated times in RPMI 1640, supplemented with antibiotics and 10% heat-inactivated FCS. In some experiments, cells were stimulated in the presence of cytokine for 3 h and replenished with cytokine-free media for

indicated times. Cells were washed in cold PBS and lysed in radioimmunoprecipitation assay buffer in the presence of protease and phosphatase inhibitors. Protein lysates were normalized with a bicinchoninic acid protein assay and samples loaded in SDS sample buffer. Protein extracts were separated on NuPAGE 4–12% Bis-Tris Protein Gel and transferred to polyvinylidene difluoride membranes. The membranes were probed with antibodies and visualized with the Immobilon Western Chemiluminescent HRP Substrate (see Table S1 for antibodies, clones, and reagents).

Surface plasmon resonance

The binding of CIS protein to phosphopeptide motifs from the β common receptor was analyzed by competition experiments using surface plasmon resonance. A biotinylated phosphotyrosine-containing peptide from JAK3 was bound to a streptavidin derivatized carboxymethyldextran chip (SAD 200 chip, Xantec) using a flow-rate of 10 µl/min for 6 min at a concentration of 10 µg/ml in a Biacore 4000. A purified recombinant ternary complex of CIS bound to elongin B and elongin C was then passed over the surface of the chip at a concentration of 125 nM to assess binding and measure the total response unit. This experiment was then repeated with the β common receptor and GM-CSFRα included as competitors to disrupt binding to the phosphopeptide on the surface of the chip. Each tyrosine-phosphorylated peptide motif from the GM-CSFR was tested for competition at concentrations of 10 µM to 41 µM (five serial threefold dilution of 10 µM). Binding was quantified by measuring the response units for each injection and plotting the results as an IC_{50} (half-maximal inhibitory concentration) curve.

Sample preparation for mass spectrometry-based proteomics

BM neutrophils from BM of C57BL/6J or $CIS^{-/-}$ mice were sorted (PI^- $CD3^-$ $CD19^-$ $CD115^-$ $CD11b^+$ $Ly6G^+$) on a FACS ARIA Fusion cell sorter (BD Biosciences) to achieve a final purity of 99–100%. Neutrophils (3×10^6) from each genotype and stimulation condition (n = 3/group) were washed three times with ice-cold PBS before dry cell pellet storage at −80°C. Cells were lysed in preheated (95°C) 5% SDS/10 mM Tris/10 mM Tris (2-carboxyethyl) phosphine/5.5 mM and 2-chloracetamide and then heated at 95°C for 10 min. Neat trifluoracetic acid (Sigma) resulting in a final concentration of 1% was added to hydrolyze DNA. Lysates were quenched with 4 M Tris (pH 10) resulting in a final concentration of ∼140 mM (pH 7). Cell lysates (∼40 µg protein) were transferred to a 2 ml LoBind Deep Well plate (Eppendorf) and prepared for mass spectrometry analysis using the SP3 protocol, as described (Hughes et al., 2014), but with some modifications. For all experiments with magnetic beads, we used a 1:1 combination mix of the two types of commercially available paramagnetic carboxylate beads (Sera-Mag Speed beads, no. 45152105050250, no. 65152105050250, Thermo Fisher Scientific). Beads were freshly prepared by rinsing with water three times before use at a stock concentration of 20 µg/µl. Carboxylate beads (4 µl) were added to all samples along with acetonitrile (ACN, 70% final concentration vol/vol) and incubated at room temperature for 18 min. Samples were then placed on a magnetic 96-well rack (Ambion, Thermo Fisher Scientific), supernatants were discarded, and the beads washed twice with 70% ethanol and once with neat ACN (180 µl washes). ACN was completely evaporated from the tubes using a CentriVap (Labconco) before the addition of 40 µl digestion buffer (10% trifluoroethanol/100 mM NH_4HCO_3) containing Lys-C (Wako, 129–02541) and Trypsin-gold (Promega, V5280), each at a 1:25 enzyme:substrate ratio. Enzymatic digestions proceeded for 1.5 h at 37°C using the ThermoMixer C (Eppendorf), shaking at 400 rpm. Following digestion, samples were placed on a magnetic rack, the supernatants containing peptides were collected, and an additional elution (50 µl) was performed using 2% DMSO (Sigma) before sonication in a water bath for 1 min. The eluates were pooled and transferred to the top of preequilibrated C18 StageTips (2× plugs of 3M Empore resin, no. 2215) for sample cleanup. The eluates were lyophilized to dryness using a CentriVap (Labconco), before reconstituting in 60 µl 0.1% FA/2% ACN ready for mass spectometry analysis.

Mass spectrometry analysis

Peptides (2 µl) were separated by reverse-phase chromatography on a C_{18} fused silica column (inner diameter 75 µm, OD 360 µm × 25 cm length, 1.6 µm C_{18} beads) packed into an emitter tip (IonOpticks), using a nano-flow HPLC (M-class, Waters). The HPLC was coupled to an Impact II UHR-QqTOF mass spectrometer (Bruker Daltonics, Bremen) using a CaptiveSpray source and nanoBooster at 0.20 Bar using ACN. Peptides were loaded directly onto the column at a constant flow rate of 400 nl/min with buffer A (99.9% Milli-Q water, 0.1% FA) and eluted with a 90-min linear gradient from 2 to 34% buffer B (99.9% ACN, 0.1% FA). Mass spectra were acquired in a data-dependent manner including an automatic switch between mass spectometry and tandem mass spectrometry scans using a 1.5-s duty cycle and 4 Hz mass spectometry 1 spectra rate followed by tandem mass spectrometry scans at 8–20 Hz dependent on precursor intensity for the remainder of the cycle. Mass spectometry spectra were acquired between a mass range of 200 and 2,000 m/z. Peptide fragmentation was performed using collision-induced dissociation. Raw files consisting of high-resolution tandem mass spectrometry spectra from the Bruker Impact II instrument were processed with MaxQuant (version 1.5.8.3) for feature detection and protein identification using the Andromeda search engine (Cox et al., 2011). Extracted peak lists were searched against the UniProtKB/Swiss-Prot *Mus musculus* database (October 2016) and a separate reverse decoy database to empirically assess the false discovery rate (FDR) using strict trypsin specificity allowing up to two missed cleavages. The minimum required peptide length was set to 7 amino acids. In the main search, precursor mass tolerance was 0.006 daltons, and fragment mass tolerance was 40 ppm. The search included variable modifications of oxidation (methionine), N-terminal acetylation, the addition of pyroglutamate (at N termini of glutamate and glutamine), and a fixed modification of carbamidomethyl (cysteine). The "match between runs" option in MaxQuant was used to transfer identifications made between runs on the basis of matching precursors with high mass accuracy (Cox and Mann, 2008). Peptide-spectrum match and protein identifications were filtered using a target-decoy

approach at an FDR of 1%. Label-free quantification (LFQ) quantification was selected, with a minimum ratio count of 2. Peptide-spectrum match scores and protein identifications were filtered using a target-decoy approach at a FDR of 1%. Only unique and razor peptides were considered for quantification with intensity values present in at least two out of three replicates per group. Statistical analyses were performed using LFQAnalyst (https://bioinformatics.erc.monash.edu/apps/LFQ-Analyst/) whereby the LFQ intensity values were used for protein quantification. Missing values were replaced by values drawn from a normal distribution of 1.8 SDs and a width of 0.3 for each sample (Perseus-type). Protein-wise linear models combined with empirical Bayes statistics were used for differential expression analysis using Bioconductor package Limma, whereby the adjusted P value cutoff was set at 0.05 and log2 fold change cutoff set at 1. The Benjamini–Hochberg method of FDR correction was used.

RNASeq

BM neutrophils from BM of C57BL/6J or CIS$^{-/-}$ mice were sorted (PI$^-$ CD3$^-$ CD19$^-$ CD115$^-$ CD11b$^+$ Ly6G$^+$) by a FACS ARIA Fusion cell sorter (BD Biosciences) to achieve a final purity of 99–100%. Neutrophils were stimulated with recombinant GM-CSF (100 ng/ml) for indicated times. RNA from neutrophils was extracted with an RNeasy Plus Mini Kit (QIAGEN), according to the manufacturer's protocol. Extracted RNA was quantified using an Agilent 2200 TapeStation System (Agilent) with RNA ScreenTapes (Agilent) or High Sensitivity RNA ScreenTapes (Agilent). Next-generation sequencing libraries were created with 100 ng of RNA from samples with distinct 18S and 28S peaks and RNA Integrity Number values greater than 7, using an NEBNext Ultra II Directional RNA Library Prep Kit for Illumina New England Biolabs) according to the manufacturer's protocol. RNA libraries were pooled and sent for single-end 75 bp sequencing at the Genomics Laboratory (The Walter and Eliza Hall Institute of Medical Research) on a NextSeq 500 next-generation sequencer (Illumina) to obtain ∼20 million reads per sample.

Bioinformatics

Single-end 75-bp reads corresponding to WT and CIS$^{-/-}$ neutrophils treated with GM-CSF in 0 (unstimulated), 4 h and 24 h time-points RNASeq samples were quality checked using fastqc (http://www.bioinformatics.babraham.ac.uk/projects/fastqc). Low-quality base pairs were trimmed from the end of the reads using Trimmomatic (Bolger et al., 2014). Reads were aligned to mm10 using STAR (Dobin et al., 2013). Reads were summarized at the gene level using featureCounts (Liao et al., 2014). The differential expression and pathway enrichment analysis were performed using edgeR (Chen et al., 2014) and limma (Ritchie et al., 2015) R/Biocondutor packages. Differential protein analysis was performed using the diffSplice function in limma. Briefly, technical variabilities and batch effects in the LFQ normalized peptide intensities from MaxQuant were estimated from a surrogate variable analysis and incorporated into the differential expression model. A protein is identified as differentially expressed if the protein-wise P values derived from the Simes-adjusted P values for its peptides is significant (FDR 0.05).

Statistics

In arthritis experiments, differences in clinical score between the groups were assessed using two-way ANOVA for repeated measurements, with Bonferroni post-test correction to compare differences between the groups. For other experiments, differences between groups were determined using unpaired Student's *t* tests, as indicated. All analyses were performed using GraphPad Prism version 7 (GraphPad Software). Data are shown as means ± SEM unless stated otherwise. Levels of statistical significance are expressed as P values: *, $P < 0.05$, **, $P < 0.01$, and ***, $P < 0.001$.

Data and materials availability

The accession number for the RNASeq reported in this paper is GEO accession no. GSE128909. The mass spectrometry proteomics data have been deposited to the ProteomeXchange Consortium via the PRIDE partner repository (Vizcaíno et al., 2016) with the dataset identifier PXD012794.

Online Supplemental material

Fig. S1 shows the generation and validation of Gr/fr mice. Fig. S2 shows flow-cytometric analyses of GM-CSF in human NK cells and T cell subsets from RA SF and peripheral blood of healthy donors. Fig. S3 shows induction of CIS in human myeloid cells by GM-CSF stimulation, the myeloid compartment of CIS$^{-/-}$ mice, and prolonged p38 MAPK and SAPK/JNK signaling in CIS$^{-/-}$ neutrophils in response to GM-CSF. Fig. S4 shows an overview of the RNASeq analysis of WT and CIS$^{-/-}$ neutrophils at various times after GM-CSF stimulation. Fig. S5 shows hyperactivation of CIS$^{-/-}$ myeloid cells in response to GM-CSF and exacerbated EAE in CIS$^{-/-}$ mice. Table S1 contains a list of reagents and software used in this study.

Acknowledgments

We thank all the members of the Wicks and Huntington Laboratories for discussion, comments, and advice on this project, The Walter and Eliza Hall Institute of Medical Research Bioservices for mouse breeding, maintenance, and technical support, and Jeanette Rientjes (Gene Recombineering Facility, Monash University), Janelle Lochland, Liz Viney, and Fiona Waters for assistance in the generation of *Csf2*$^{fl/fl}$ mice. We thank Prof. Marc Pellegrini (The Walter and Eliza Hall Institute of Medical Research, Parkville, Australia) for providing IFN-γ$^{-/-}$ mice and Prof. Burkhard Becher (Institute of Experimental Immunology, University of Zurich, Zurich, Switzerland) for *Csf2rb*$^{fl/fl}$ mice.

This work is supported by grants from the National Health and Medical Research Council of Australia (1113577 to W.S. Alexander and I.P. Wicks; 1124784, 1066770, 1057852, and 1124907 to N.D. Huntington; and 1140406 to F. Souza-Fonseca-Guimaraes) and John T. Reid Charitable Trusts to I.P. Wicks. I.P. Wicks is supported by a National Health and Medical Research Council Medical Research Future Fund Practitioner Fellowship (1154325). F. Souza-Fonseca-Guimaraes was supported by a National Health

and Medical Research Council Early Career Fellowship (1088703), a National Breast Cancer Foundation Fellowship (PF-15-008), and grant awarded through the Priority-Driven Collaborative Cancer Research Scheme (1120725) and funded by Cure Cancer Australia Foundation with the assistance of Cancer Australia. N.D. Huntington is a National Health and Medical Research Council CDF2 Fellow (1124788), a recipient of a Melanoma Research Grant from the Harry J. Lloyd Charitable Trust, a Melanoma Research Alliance Young Investigator Award, a Tour De Cure research grant, an equipment grant from the Ian Potter Foundation, and a CLIP grant from the Cancer Research Institute. W.S. Alexander is a National Health and Medical Research Council Senior Principal Research Fellow (1058344). This study was made possible through Victorian State Government Operational Infrastructure Support and the Australian Government National Health and Medical Research Council Independent Research Institute Infrastructure Support scheme.

Author contributions: Conceptualization, C. Louis, F. Souza-Fonseca-Guimaraes, N.D. Huntington, and I.P. Wicks; investigation, C. Louis, F. Souza-Fonseca-Guimaraes, Y. Yang, D. D'Silva, T. Kratina, L. Dagley, S. Hediyeh-Zadeh, J. Rautela, S.L. Masters, M.J. Davis, J.J. Babon, and W.S. Alexander; writing (original draft), C. Louis; manuscript revision, F. Souza-Fonseca-Guimaraes, N.D. Huntington, and I.P. Wicks; funding acquisition, F. Souza-Fonseca-Guimaraes, N.D. Huntington, W.S. Alexander, and I.P. Wicks; resources, B. Ciric, L. Dagley, S. Hediyeh-Zadeh, J. Rautela, S.L. Masters, M.J. Davis, J.J. Babon, E. Vivier, W.S. Alexander, N.D. Huntington, and I.P. Wicks; supervision, C. Louis, F. Souza-Fonseca-Guimaraes, N.D. Huntington, and I.P. Wicks.

Disclosures: Dr. Rautela is the co-founder and CEO of oNKo-innate Pty. Ltd. Dr. Masters reported personal fees from IFM Therapeutics, personal fees from Quench Bio, and grants from GlaxoSmithKline outside the submitted work. Dr. Babon reported a patent to inhibition of cytokine-induced sh2 protein in NK cells, licensed "Servier." Dr. Vivier reported personal fees from Innate Pharma during the conduct of the study; personal fees from Innate Pharma outside the submitted work; and is an employee of Innate Pharma. Dr. Huntington reported "other" from Servier during the conduct of the study; personal fees from ONKo-Innate outside the submitted work; has a patent to WO201700861A1 with royalties paid, Servier; and is the founder of oNKo-Innate Pty Ltd. Dr. Wicks reported, "I have argued that GM-CSF is an important therapeutic target in inflammatory diseases (see Wicks and Roberts, Nature Reviews Rheumatology 2016) and have provided advice around clinical translation to several companies interested in the area, namely Medimmune and Kiniksa. I have no relevant IP and these companies were not involved in the project described in our submission to JEM, nor did they provide funding. I don't believe there is any conflict of interest, but declare it because I have been an advocate for therapeutic antagonism of GM-CSF." No other disclosures were reported.

Submitted: 31 July 2019
Revised: 25 November 2019
Accepted: 15 January 2020

References

Achuthan, A., A.D. Cook, M.C. Lee, R. Saleh, H.W. Khiew, M.W. Chang, C. Louis, A.J. Fleetwood, D.C. Lacey, A.D. Christensen, et al. 2016. Granulocyte macrophage colony-stimulating factor induces CCL17 production via IRF4 to mediate inflammation. *J. Clin. Invest.* 126:3453–3466. https://doi.org/10.1172/JCI87828

Al-Mossawi, M.H., L. Chen, H. Fang, A. Ridley, J. de Wit, N. Yager, A. Hammitzsch, I. Pulyakhina, B.P. Fairfax, D. Simone, et al. 2017. Unique transcriptome signatures and GM-CSF expression in lymphocytes from patients with spondyloarthritis. *Nat. Commun.* 8:1510. https://doi.org/10.1038/s41467-017-01771-2

Alvaro-Gracia, J.M., N.J. Zvaifler, C.B. Brown, K. Kaushansky, and G.S. Firestein. 1991. Cytokines in chronic inflammatory arthritis. VI. Analysis of the synovial cells involved in granulocyte-macrophage colony-stimulating factor production and gene expression in rheumatoid arthritis and its regulation by IL-1 and tumor necrosis factor-alpha. *J. Immunol.* 146:3365–3371.

Anzai, A., J.L. Choi, S. He, A.M. Fenn, M. Nairz, S. Rattik, C.S. McAlpine, J.E. Mindur, C.T. Chan, Y. Iwamoto, et al. 2017. The infarcted myocardium solicits GM-CSF for the detrimental oversupply of inflammatory leukocytes. *J. Exp. Med.* 214:3293–3310. https://doi.org/10.1084/jem.20170689

Bär, E., P.G. Whitney, K. Moor, C. Reis e Sousa, and S. LeibundGut-Landmann. 2014. IL-17 regulates systemic fungal immunity by controlling the functional competence of NK cells. *Immunity.* 40:117–127. https://doi.org/10.1016/j.immuni.2013.12.002

Becher, B., S. Tugues, and M. Greter. 2016. GM-CSF: From Growth Factor to Central Mediator of Tissue Inflammation. *Immunity.* 45:963–973. https://doi.org/10.1016/j.immuni.2016.10.026

Bolger, A.M., M. Lohse, and B. Usadel. 2014. Trimmomatic: a flexible trimmer for Illumina sequence data. *Bioinformatics.* 30:2114–2120. https://doi.org/10.1093/bioinformatics/btu170

Brady, J., S. Carotta, R.P. Thong, C.J. Chan, Y. Hayakawa, M.J. Smyth, and S.L. Nutt. 2010. The interactions of multiple cytokines control NK cell maturation. *J. Immunol.* 185:6679–6688. https://doi.org/10.4049/jimmunol.0903354

Bramwell, K.K., Y. Ma, J.H. Weis, X. Chen, J.F. Zachary, C. Teuscher, and J.J. Weis. 2014. Lysosomal β-glucuronidase regulates Lyme and rheumatoid arthritis severity. *J. Clin. Invest.* 124:311–320. https://doi.org/10.1172/JCI72339

Bramwell, K.K., K. Mock, Y. Ma, J.H. Weis, C. Teuscher, and J.J. Weis. 2015. β-Glucuronidase, a Regulator of Lyme Arthritis Severity, Modulates Lysosomal Trafficking and MMP-9 Secretion in Response to Inflammatory Stimuli. *J. Immunol.* 195:1647–1656. https://doi.org/10.4049/jimmunol.1500212

Bunda, S., K. Kommaraju, P. Heir, and M. Ohh. 2013. SOCS-1 mediates ubiquitylation and degradation of GM-CSF receptor. *PLoS One.* 8:e76370. https://doi.org/10.1371/journal.pone.0076370

Burmester, G.R., I.B. McInnes, J. Kremer, P. Miranda, M. Korkosz, J. Vencovsky, A. Rubbert-Roth, E. Mysler, M.A. Sleeman, A. Godwood, et al. EARTH EXPLORER 1 study investigators. 2017. A randomised phase IIb study of mavrilimumab, a novel GM-CSF receptor alpha monoclonal antibody, in the treatment of rheumatoid arthritis. *Ann. Rheum. Dis.* 76:1020–1030. https://doi.org/10.1136/annrheumdis-2016-210624

Burmester, G.R., I.B. McInnes, J.M. Kremer, P. Miranda, J. Vencovský, A. Godwood, M. Albulescu, M.A. Michaels, X. Guo, D. Close, and M. Weinblatt. 2018. Mavrilimumab, a Fully Human Granulocyte-Macrophage Colony-Stimulating Factor Receptor α Monoclonal Antibody: Long-Term Safety and Efficacy in Patients With Rheumatoid Arthritis. *Arthritis Rheumatol.* 70:679–689. https://doi.org/10.1002/art.40420

Burnham, M.E., C.J. Koziol-White, S. Esnault, M.E. Bates, M.D. Evans, P.J. Bertics, and L.C. Denlinger. 2013. Human airway eosinophils exhibit preferential reduction in STAT signaling capacity and increased CISH expression. *J. Immunol.* 191:2900–2906. https://doi.org/10.4049/jimmunol.1300297

Caligiuri, M.A. 2008. Human natural killer cells. *Blood.* 112:461–469. https://doi.org/10.1182/blood-2007-09-077438

Campbell, I.K., M.J. Rich, R.J. Bischof, A.R. Dunn, D. Grail, and J.A. Hamilton. 1998. Protection from collagen-induced arthritis in granulocyte-macrophage colony-stimulating factor-deficient mice. *J. Immunol.* 161:3639–3644.

Chamberlain, N.D., S.J. Kim, O.M. Vila, M.V. Volin, S. Volkov, R.M. Pope, S. Arami, A.M. Mandelin II, and S. Shahrara. 2013. Ligation of TLR7 by rheumatoid arthritis synovial fluid single strand RNA induces

transcription of TNFα in monocytes. *Ann. Rheum. Dis.* 72:418–426. https://doi.org/10.1136/annrheumdis-2011-201203

Chen, Y.S., A.T.L. Lun, and G.K. Smyth. 2014. Differential Expression Analysis of Complex RNA-seq Experiments Using edgeR. *In* Statistical Analysis of Next Generation Sequencing Data. S. Datta, and D. Nettleton, editors. Springer. pp. 51–74. https://doi.org/10.1007/978-3-319-07212-8_3

Choe, J.Y., B. Crain, S.R. Wu, and M. Corr. 2003. Interleukin 1 receptor dependence of serum transferred arthritis can be circumvented by toll-like receptor 4 signaling. *J. Exp. Med.* 197:537–542. https://doi.org/10.1084/jem.20021850

Chou, R.C., N.D. Kim, C.D. Sadik, E. Seung, Y. Lan, M.H. Byrne, B. Haribabu, Y. Iwakura, and A.D. Luster. 2010. Lipid-cytokine-chemokine cascade drives neutrophil recruitment in a murine model of inflammatory arthritis. *Immunity.* 33:266–278. https://doi.org/10.1016/j.immuni.2010.07.018

Christmas, P., S.R. Ursino, J.W. Fox, and R.J. Soberman. 1999. Expression of the CYP4F3 gene. tissue-specific splicing and alternative promoters generate high and low K(m) forms of leukotriene B(4) omega-hydroxylase. *J. Biol. Chem.* 274:21191–21199. https://doi.org/10.1074/jbc.274.30.21191

Codarri, L., G. Gyülvészi, V. Tosevski, L. Hesske, A. Fontana, L. Magnenat, T. Suter, and B. Becher. 2011. RORγt drives production of the cytokine GM-CSF in helper T cells, which is essential for the effector phase of autoimmune neuroinflammation. *Nat. Immunol.* 12:560–567. https://doi.org/10.1038/ni.2027

Cook, A.D., A.L. Turner, E.L. Braine, J. Pobjoy, J.C. Lenzo, and J.A. Hamilton. 2011. Regulation of systemic and local myeloid cell subpopulations by bone marrow cell-derived granulocyte-macrophage colony-stimulating factor in experimental inflammatory arthritis. *Arthritis Rheum.* 63:2340–2351. https://doi.org/10.1002/art.30354

Corren, J. 2011. Anti-interleukin-5 antibody therapy in asthma and allergies. *Curr. Opin. Allergy Clin. Immunol.* 11:565–570. https://doi.org/10.1097/ACI.0b013e32834c3d30

Cox, J., and M. Mann. 2008. MaxQuant enables high peptide identification rates, individualized p.p.b.-range mass accuracies and proteome-wide protein quantification. *Nat. Biotechnol.* 26:1367–1372. https://doi.org/10.1038/nbt.1511

Cox, J.H., A.E. Starr, R. Kappelhoff, R. Yan, C.R. Roberts, and C.M. Overall. 2010. Matrix metalloproteinase 8 deficiency in mice exacerbates inflammatory arthritis through delayed neutrophil apoptosis and reduced caspase 11 expression. *Arthritis Rheum.* 62:3645–3655. https://doi.org/10.1002/art.27757

Cox, J., N. Neuhauser, A. Michalski, R.A. Scheltema, J.V. Olsen, and M. Mann. 2011. Andromeda: a peptide search engine integrated into the MaxQuant environment. *J. Proteome Res.* 10:1794–1805. https://doi.org/10.1021/pr101065j

Croker, B.A., D. Metcalf, L. Robb, W. Wei, S. Mifsud, L. DiRago, L.A. Cluse, K.D. Sutherland, L. Hartley, E. Williams, et al. 2004. SOCS3 is a critical physiological negative regulator of G-CSF signaling and emergency granulopoiesis. *Immunity.* 20:153–165. https://doi.org/10.1016/S1074-7613(04)00022-6

Croxford, A.L., M. Lanzinger, F.J. Hartmann, B. Schreiner, F. Mair, P. Pelczar, B.E. Clausen, S. Jung, M. Greter, and B. Becher. 2015. The Cytokine GM-CSF Drives the Inflammatory Signature of CCR2+ Monocytes and Licenses Autoimmunity. *Immunity.* 43:502–514. https://doi.org/10.1016/j.immuni.2015.08.010

Cuturi, M.C., I. Anegón, F. Sherman, R. Loudon, S.C. Clark, B. Perussia, and G. Trinchieri. 1989. Production of hematopoietic colony-stimulating factors by human natural killer cells. *J. Exp. Med.* 169:569–583. https://doi.org/10.1084/jem.169.2.569

Dalbeth, N., and M.F. Callan. 2002. A subset of natural killer cells is greatly expanded within inflamed joints. *Arthritis Rheum.* 46:1763–1772. https://doi.org/10.1002/art.10410

Dalton, D.K., S. Pitts-Meek, S. Keshav, I.S. Figari, A. Bradley, and T.A. Stewart. 1993. Multiple defects of immune cell function in mice with disrupted interferon-gamma genes. *Science.* 259:1739–1742. https://doi.org/10.1126/science.8456300

Del Prete, A., L. Martínez-Muñoz, C. Mazzon, L. Toffali, F. Sozio, L. Za, D. Bosisio, L. Gazzurelli, V. Salvi, L. Tiberio, et al. 2017. The atypical receptor CCRL2 is required for CXCR2-dependent neutrophil recruitment and tissue damage. *Blood.* 130:1223–1234. https://doi.org/10.1182/blood-2017-04-777680

Delconte, R.B., T.B. Kolesnik, L.F. Dagley, J. Rautela, W. Shi, E.M. Putz, K. Stannard, J.G. Zhang, C. Teh, M. Firth, et al. 2016. CIS is a potent checkpoint in NK cell-mediated tumor immunity. *Nat. Immunol.* 17:816–824. https://doi.org/10.1038/ni.3470

Dobin, A., C.A. Davis, F. Schlesinger, J. Drenkow, C. Zaleski, S. Jha, P. Batut, M. Chaisson, and T.R. Gingeras. 2013. STAR: ultrafast universal RNA-seq aligner. *Bioinformatics.* 29:15–21. https://doi.org/10.1093/bioinformatics/bts635

Domínguez-Andrés, J., L. Feo-Lucas, M. Minguito de la Escalera, L. González, M. López-Bravo, and C. Ardavín. 2017. Inflammatory Ly6C^{high} Monocytes Protect against Candidiasis through IL-15-Driven NK Cell/Neutrophil Activation. *Immunity.* 46:1059–1072.e4. https://doi.org/10.1016/j.immuni.2017.05.009

Duffau, P., H. Menn-Josephy, C.M. Cuda, S. Dominguez, T.R. Aprahamian, A.A. Watkins, K. Yasuda, P. Monach, R. Lafyatis, L.M. Rice, et al. 2015. Promotion of Inflammatory Arthritis by Interferon Regulatory Factor 5 in a Mouse Model. *Arthritis Rheumatol.* 67:3146–3157. https://doi.org/10.1002/art.39321

El-Behi, M., B. Ciric, H. Dai, Y. Yan, M. Cullimore, F. Safavi, G.X. Zhang, B.N. Dittel, and A. Rostami. 2011. The encephalitogenicity of T(H)17 cells is dependent on IL-1- and IL-23-induced production of the cytokine GM-CSF. *Nat. Immunol.* 12:568–575. https://doi.org/10.1038/ni.2031

Esashi, E., Y.H. Wang, O. Perng, X.F. Qin, Y.J. Liu, and S.S. Watowich. 2008. The signal transducer STAT5 inhibits plasmacytoid dendritic cell development by suppressing transcription factor IRF8. *Immunity.* 28:509–520. https://doi.org/10.1016/j.immuni.2008.02.013

Farley, F.W., P. Soriano, L.S. Steffen, and S.M. Dymecki. 2000. Widespread recombinase expression using FLPeR (flipper) mice. *Genesis.* 28:106–110. https://doi.org/10.1002/1526-968X(200011/12)28:3/4<106::AID-GENE30>3.0.CO;2-T

García, S., J. Forteza, C. López-Otin, J.J. Gómez-Reino, A. González, and C. Conde. 2010. Matrix metalloproteinase-8 deficiency increases joint inflammation and bone erosion in the K/BxN serum-transfer arthritis model. *Arthritis Res. Ther.* 12:R224. https://doi.org/10.1186/ar3211

Gracie, J.A., R.J. Forsey, W.L. Chan, A. Gilmour, B.P. Leung, M.R. Greer, K. Kennedy, R. Carter, X.Q. Wei, D. Xu, et al. 1999. A proinflammatory role for IL-18 in rheumatoid arthritis. *J. Clin. Invest.* 104:1393–1401. https://doi.org/10.1172/JCI7317

Griseri, T., I.C. Arnold, C. Pearson, T. Krausgruber, C. Schiering, F. Franchini, J. Schulthess, B.S. McKenzie, P.R. Crocker, and F. Powrie. 2015. Granulocyte Macrophage Colony-Stimulating Factor-Activated Eosinophils Promote Interleukin-23 Driven Chronic Colitis. *Immunity.* 43:187–199. https://doi.org/10.1016/j.immuni.2015.07.008

Guedez, Y.B., K.B. Whittington, J.L. Clayton, L.A. Joosten, F.A. van de Loo, W.B. van den Berg, and E.F. Rosloniec. 2001. Genetic ablation of interferon-gamma up-regulates interleukin-1beta expression and enables the elicitation of collagen-induced arthritis in a nonsusceptible mouse strain. *Arthritis Rheum.* 44:2413–2424. https://doi.org/10.1002/1529-0131(200110)44:10<2413::AID-ART406>3.0.CO;2-E

Guilliams, M., I. De Kleer, S. Henri, S. Post, L. Vanhoutte, S. De Prijck, K. Deswarte, B. Malissen, H. Hammad, and B.N. Lambrecht. 2013. Alveolar macrophages develop from fetal monocytes that differentiate into long-lived cells in the first week of life via GM-CSF. *J. Exp. Med.* 210:1977–1992. https://doi.org/10.1084/jem.20131199

Haak, S., A.L. Croxford, K. Kreymborg, F.L. Heppner, S. Pouly, B. Becher, and A. Waisman. 2009. IL-17A and IL-17F do not contribute vitally to autoimmune neuro-inflammation in mice. *J. Clin. Invest.* 119:61–69.

Helft, J., J. Böttcher, P. Chakravarty, S. Zelenay, J. Huotari, B.U. Schraml, D. Goubau, and C. Reis e Sousa. 2015. GM-CSF Mouse Bone Marrow Cultures Comprise a Heterogeneous Population of CD11c(+)MHCII(+) Macrophages and Dendritic Cells. *Immunity.* 42:1197–1211. https://doi.org/10.1016/j.immuni.2015.05.018

Hesslein, D.G., R. Takaki, M.L. Hermiston, A. Weiss, and L.L. Lanier. 2006. Dysregulation of signaling pathways in CD45-deficient NK cells leads to differentially regulated cytotoxicity and cytokine production. *Proc. Natl. Acad. Sci. USA.* 103:7012–7017. https://doi.org/10.1073/pnas.0601851103

Hirota, K., M. Hashimoto, Y. Ito, M. Matsuura, H. Ito, M. Tanaka, H. Watanabe, G. Kondoh, A. Tanaka, K. Yasuda, et al. 2018. Autoimmune Th17 Cells Induced Synovial Stromal and Innate Lymphoid Cell Secretion of the Cytokine GM-CSF to Initiate and Augment Autoimmune Arthritis. *Immunity.* 48:1220–1232.e5. https://doi.org/10.1016/j.immuni.2018.04.009

Ho, E.L., L.N. Carayannopoulos, J. Poursine-Laurent, J. Kinder, B. Plougastel, H.R. Smith, and W.M. Yokoyama. 2002. Costimulation of multiple NK cell activation receptors by NKG2D. *J. Immunol.* 169:3667–3675. https://doi.org/10.4049/jimmunol.169.7.3667

Hughes, C.S., S. Foehr, D.A. Garfield, E.E. Furlong, L.M. Steinmetz, and J. Krijgsveld. 2014. Ultrasensitive proteome analysis using paramagnetic

bead technology. *Mol. Syst. Biol.* 10:757. https://doi.org/10.15252/msb.20145625

Huntington, N.D., Y. Xu, S.L. Nutt, and D.M. Tarlinton. 2005. A requirement for CD45 distinguishes Ly49D-mediated cytokine and chemokine production from killing in primary natural killer cells. *J. Exp. Med.* 201:1421–1433. https://doi.org/10.1084/jem.20042294

Inglis, J.J., E. Simelyte, F.E. McCann, G. Criado, and R.O. Williams. 2008. Protocol for the induction of arthritis in C57BL/6 mice. *Nat. Protoc.* 3:612–618. https://doi.org/10.1038/nprot.2008.19

Jackson, S.H., C.R. Yu, R.M. Mahdi, S. Ebong, and C.E. Egwuagu. 2004. Dendritic cell maturation requires STAT1 and is under feedback regulation by suppressors of cytokine signaling. *J. Immunol.* 172:2307–2315. https://doi.org/10.4049/jimmunol.172.4.2307

Jacobs, J.P., A. Ortiz-Lopez, J.J. Campbell, C.J. Gerard, D. Mathis, and C. Benoist. 2010. Deficiency of CXCR2, but not other chemokine receptors, attenuates autoantibody-mediated arthritis in a murine model. *Arthritis Rheum.* 62:1921–1932.

Ji, H., K. Ohmura, U. Mahmood, D.M. Lee, F.M. Hofhuis, S.A. Boackle, K. Takahashi, V.M. Holers, M. Walport, C. Gerard, et al. 2002a. Arthritis critically dependent on innate immune system players. *Immunity.* 16:157–168. https://doi.org/10.1016/S1074-7613(02)00275-3

Ji, H., A. Pettit, K. Ohmura, A. Ortiz-Lopez, V. Duchatelle, C. Degott, E. Gravallese, D. Mathis, and C. Benoist. 2002b. Critical roles for interleukin 1 and tumor necrosis factor alpha in antibody-induced arthritis. *J. Exp. Med.* 196:77–85. https://doi.org/10.1084/jem.20020439

Kim, S.J., Z. Chen, A.B. Essani, H.A. Elshabrawy, M.V. Volin, S. Volkov, W. Swedler, S. Arami, N. Sweiss, and S. Shahrara. 2016. Identification of a Novel Toll-like Receptor 7 Endogenous Ligand in Rheumatoid Arthritis Synovial Fluid That Can Provoke Arthritic Joint Inflammation. *Arthritis Rheumatol.* 68:1099–1110.

Komuczki, J., S. Tuzlak, E. Friebel, T. Hartwig, S. Spath, P. Rosenstiel, A. Waisman, L. Opitz, M. Oukka, B. Schreiner, et al. 2019. Fate-Mapping of GM-CSF Expression Identifies a Discrete Subset of Inflammation-Driving T Helper Cells Regulated by Cytokines IL-23 and IL-1β. *Immunity.* 50:1289–1304.e6. https://doi.org/10.1016/j.immuni.2019.04.006

Korganow, A.S., H. Ji, S. Mangialaio, V. Duchatelle, R. Pelanda, T. Martin, C. Degott, H. Kikutani, K. Rajewsky, J.L. Pasquali, et al. 1999. From systemic T cell self-reactivity to organ-specific autoimmune disease via immunoglobulins. *Immunity.* 10:451–461. https://doi.org/10.1016/S1074-7613(00)80045-X

Lalor, S.J., L.S. Dungan, C.E. Sutton, S.A. Basdeo, J.M. Fletcher, and K.H. Mills. 2011. Caspase-1-processed cytokines IL-1beta and IL-18 promote IL-17 production by gammadelta and CD4 T cells that mediate autoimmunity. *J. Immunol.* 186:5738–5748. https://doi.org/10.4049/jimmunol.1003597

Leavenworth, J.W., X. Wang, C.S. Wenander, P. Spee, and H. Cantor. 2011. Mobilization of natural killer cells inhibits development of collagen-induced arthritis. *Proc. Natl. Acad. Sci. USA.* 108:14584–14589. https://doi.org/10.1073/pnas.1112188108

Liao, Y., G.K. Smyth, and W. Shi. 2014. featureCounts: an efficient general purpose program for assigning sequence reads to genomic features. *Bioinformatics.* 30:923–930. https://doi.org/10.1093/bioinformatics/btt656

Lo, C.K., Q.L. Lam, L. Sun, S. Wang, K.H. Ko, H. Xu, C.Y. Wu, B.J. Zheng, and L. Lu. 2008. Natural killer cell degeneration exacerbates experimental arthritis in mice via enhanced interleukin-17 production. *Arthritis Rheum.* 58:2700–2711. https://doi.org/10.1002/art.23760

Madera, S., and J.C. Sun. 2015. Cutting edge: stage-specific requirement of IL-18 for antiviral NK cell expansion. *J. Immunol.* 194:1408–1412. https://doi.org/10.4049/jimmunol.1402001

Mantovani, A., C.A. Dinarello, M. Molgora, and C. Garlanda. 2019. Interleukin-1 and Related Cytokines in the Regulation of Inflammation and Immunity. *Immunity.* 50:778–795. https://doi.org/10.1016/j.immuni.2019.03.012

Matsumoto, A., M. Masuhara, K. Mitsui, M. Yokouchi, M. Ohtsubo, H. Misawa, A. Miyajima, and A. Yoshimura. 1997. CIS, a cytokine inducible SH2 protein, is a target of the JAK-STAT5 pathway and modulates STAT5 activation. *Blood.* 89:3148–3154. https://doi.org/10.1182/blood.V89.9.3148

McQualter, J.L., R. Darwiche, C. Ewing, M. Onuki, T.W. Kay, J.A. Hamilton, H.H. Reid, and C.C. Bernard. 2001. Granulocyte macrophage colony-stimulating factor: a new putative therapeutic target in multiple sclerosis. *J. Exp. Med.* 194:873–882. https://doi.org/10.1084/jem.194.7.873

Miah, M.A., C.-H. Yoon, J. Kim, J. Jang, Y.-R. Seong, and Y.-S. Bae. 2012. CISH is induced during DC development and regulates DC-mediated CTL activation. *Eur. J. Immunol.* In press. https://doi.org/https://doi.org/10.1002/eji.201141846

Misharin, A.V., C.M. Cuda, R. Saber, J.D. Turner, A.K. Gierut, G.K. Haines III, S. Berdnikovs, A. Filer, A.R. Clark, C.D. Buckley, et al. 2014. Nonclassical Ly6C(-) monocytes drive the development of inflammatory arthritis in mice. *Cell Reports.* 9:591–604. https://doi.org/10.1016/j.celrep.2014.09.032

Monach, P.A., D. Mathis, and C. Benoist. 2008. The K/BxN arthritis model. *Curr. Protoc. Immunol.* Chapter 15:22. https://doi.org/10.1002/0471142735.im1522s81

Morris, R., N.J. Kershaw, and J.J. Babon. 2018. The molecular details of cytokine signaling via the JAK/STAT pathway. *Protein Sci.* 27:1984–2009. https://doi.org/10.1002/pro.3519

Narni-Mancinelli, E., J. Chaix, A. Fenis, Y.M. Kerdiles, N. Yessaad, A. Reynders, C. Gregoire, H. Luche, S. Ugolini, E. Tomasello, et al. 2011. Fate mapping analysis of lymphoid cells expressing the NKp46 cell surface receptor. *Proc. Natl. Acad. Sci. USA.* 108:18324–18329. https://doi.org/10.1073/pnas.1112064108

Nigrovic, P.A., and D.M. Lee. 2007. Synovial mast cells: role in acute and chronic arthritis. *Immunol. Rev.* 217:19–37. https://doi.org/10.1111/j.1600-065X.2007.00506.x

Noster, R., R. Riedel, M.F. Mashreghi, H. Radbruch, L. Harms, C. Haftmann, H.D. Chang, A. Radbruch, and C.E. Zielinski. 2014. IL-17 and GM-CSF expression are antagonistically regulated by human T helper cells. *Sci. Transl. Med.* 6:241ra80. https://doi.org/10.1126/scitranslmed.3008706

Okada, Y., C. Terao, K. Ikari, Y. Kochi, K. Ohmura, A. Suzuki, T. Kawaguchi, E.A. Stahl, F.A. Kurreeman, N. Nishida, et al. 2012. Meta-analysis identifies nine new loci associated with rheumatoid arthritis in the Japanese population. *Nat. Genet.* 44:511–516. https://doi.org/10.1038/ng.2231

Ostberg, T., K. Kawane, S. Nagata, H. Yang, S. Chavan, L. Klevenvall, M.E. Bianchi, H.E. Harris, U. Andersson, and K. Palmblad. 2010. Protective targeting of high mobility group box chromosomal protein 1 in a spontaneous arthritis model. *Arthritis Rheum.* 62:2963–2972. https://doi.org/10.1002/art.27590

Palmer, D.C., G.C. Guittard, Z. Franco, J.G. Crompton, R.L. Eil, S.J. Patel, Y. Ji, N. Van Panhuys, C.A. Klebanoff, M. Sukumar, et al. 2015. Cish actively silences TCR signaling in CD8+ T cells to maintain tumor tolerance. *J. Exp. Med.* 212:2095–2113. https://doi.org/10.1084/jem.20150304

Passegué, E., E.F. Wagner, and I.L. Weissman. 2004. JunB deficiency leads to a myeloproliferative disorder arising from hematopoietic stem cells. *Cell.* 119:431–443. https://doi.org/10.1016/j.cell.2004.10.010

Plater-Zyberk, C., L.A. Joosten, M.M. Helsen, P. Sattonnet-Roche, C. Siegfried, S. Alouani, F.A. van De Loo, P. Graber, S. Aloni, R. Cirillo, et al. 2001. Therapeutic effect of neutralizing endogenous IL-18 activity in the collagen-induced model of arthritis. *J. Clin. Invest.* 108:1825–1832. https://doi.org/10.1172/JCI200112097

Pridgeon, C., G.P. Lennon, L. Pazmany, R.N. Thompson, S.E. Christmas, and R.J. Moots. 2003. Natural killer cells in the synovial fluid of rheumatoid arthritis patients exhibit a CD56bright,CD94bright,CD158negative phenotype. *Rheumatology (Oxford).* 42:870–878. https://doi.org/10.1093/rheumatology/keg240

Rauch, P.J., A. Chudnovskiy, C.S. Robbins, G.F. Weber, M. Etzrodt, I. Hilgendorf, E. Tiglao, J.L. Figueiredo, Y. Iwamoto, I. Theurl, et al. 2012. Innate response activator B cells protect against microbial sepsis. *Science.* 335:597–601. https://doi.org/10.1126/science.1215173

Reynolds, G., J.R. Gibbon, A.G. Pratt, M.J. Wood, D. Coady, G. Raftery, A.R. Lorenzi, A. Gray, A. Filer, C.D. Buckley, et al. 2016. Synovial CD4+ T-cell-derived GM-CSF supports the differentiation of an inflammatory dendritic cell population in rheumatoid arthritis. *Ann. Rheum. Dis.* 75:899–907. https://doi.org/10.1136/annrheumdis-2014-206578

Ritchie, M.E., B. Phipson, D. Wu, Y. Hu, C.W. Law, W. Shi, and G.K. Smyth. 2015. limma powers differential expression analyses for RNA-sequencing and microarray studies. *Nucleic Acids Res.* 43:e47. https://doi.org/10.1093/nar/gkv007

Sadik, C.D., N.D. Kim, Y. Iwakura, and A.D. Luster. 2012. Neutrophils orchestrate their own recruitment in murine arthritis through C5aR and FcγR signaling. *Proc. Natl. Acad. Sci. USA.* 109:E3177–E3185. https://doi.org/10.1073/pnas.1213797109

Sathe, P., R.B. Delconte, F. Souza-Fonseca-Guimaraes, C. Seillet, M. Chopin, C.J. Vandenberg, L.C. Rankin, L.A. Mielke, I. Vikstrom, T.B. Kolesnik, et al. 2014. Innate immunodeficiency following genetic ablation of Mcl1 in natural killer cells. *Nat. Commun.* 5:4539. https://doi.org/10.1038/ncomms5539

Schleinitz, N., F. Vély, J.R. Harlé, and E. Vivier. 2010. Natural killer cells in human autoimmune diseases. *Immunology.* 131:451–458. https://doi.org/10.1111/j.1365-2567.2010.03360.x

Smolen, J.S., D. Aletaha, and I.B. McInnes. 2016. Rheumatoid arthritis. *Lancet.* 388:2023–2038. https://doi.org/10.1016/S0140-6736(16)30173-8

Söderström, K., E. Stein, P. Colmenero, U. Purath, U. Müller-Ladner, C.T. de Matos, I.H. Tarner, W.H. Robinson, and E.G. Engleman. 2010. Natural killer cells trigger osteoclastogenesis and bone destruction in arthritis. *Proc. Natl. Acad. Sci. USA.* 107:13028–13033. https://doi.org/10.1073/pnas.1000546107

Sokolove, J., X. Zhao, P.E. Chandra, and W.H. Robinson. 2011. Immune complexes containing citrullinated fibrinogen costimulate macrophages via Toll-like receptor 4 and Fcγ receptor. *Arthritis Rheum.* 63: 53–62. https://doi.org/10.1002/art.30081

Souza-Fonseca-Guimaraes, F., M. Adib-Conquy, and J.M. Cavaillon. 2012. Natural killer (NK) cells in antibacterial innate immunity: angels or devils? *Mol. Med.* 18:270–285. https://doi.org/10.2119/molmed.2011.00201

Stanley, E., G.J. Lieschke, D. Grail, D. Metcalf, G. Hodgson, J.A. Gall, D.W. Maher, J. Cebon, V. Sinickas, and A.R. Dunn. 1994. Granulocyte/macrophage colony-stimulating factor-deficient mice show no major perturbation of hematopoiesis but develop a characteristic pulmonary pathology. *Proc. Natl. Acad. Sci. USA.* 91:5592–5596. https://doi.org/10.1073/pnas.91.12.5592

Stock, A.T., J.A. Hansen, M.A. Sleeman, B.S. McKenzie, and I.P. Wicks. 2016. GM-CSF primes cardiac inflammation in a mouse model of Kawasaki disease. *J. Exp. Med.* 213:1983–1998. https://doi.org/10.1084/jem.20151853

Svensson, L., J. Jirholt, R. Holmdahl, and L. Jansson. 1998. B cell-deficient mice do not develop type II collagen-induced arthritis (CIA). *Clin. Exp. Immunol.* 111:521–526. https://doi.org/10.1046/j.1365-2249.1998.00529.x

Syversen, S.W., P.I. Gaarder, G.L. Goll, S. Ødegård, E.A. Haavardsholm, P. Mowinckel, D. van der Heijde, R. Landewé, and T.K. Kvien. 2008. High anti-cyclic citrullinated peptide levels and an algorithm of four variables predict radiographic progression in patients with rheumatoid arthritis: results from a 10-year longitudinal study. *Ann. Rheum. Dis.* 67: 212–217. https://doi.org/10.1136/ard.2006.068247

Takeda, K., H. Tsutsui, T. Yoshimoto, O. Adachi, N. Yoshida, T. Kishimoto, H. Okamura, K. Nakanishi, and S. Akira. 1998. Defective NK cell activity and Th1 response in IL-18-deficient mice. *Immunity.* 8:383–390. https://doi.org/10.1016/S1074-7613(00)80543-9

van Lent, P.L., L. Grevers, A.B. Blom, A. Sloetjes, J.S. Mort, T. Vogl, W. Nacken, W.B. van den Berg, and J. Roth. 2008. Myeloid-related proteins S100A8/S100A9 regulate joint inflammation and cartilage destruction during antigen-induced arthritis. *Ann. Rheum. Dis.* 67:1750–1758. https://doi.org/10.1136/ard.2007.077800

van Lent, P.L., L.C. Grevers, R. Schelbergen, A. Blom, J. Geurts, A. Sloetjes, T. Vogl, J. Roth, and W.B. van den Berg. 2010. S100A8 causes a shift toward expression of activatory Fcγ receptors on macrophages via toll-like receptor 4 and regulates Fcγ receptor expression in synovium during chronic experimental arthritis. *Arthritis Rheum.* 62:3353–3364. https://doi.org/10.1002/art.27654

Vier, J., M. Groth, M. Sochalska, and S. Kirschnek. 2016. The anti-apoptotic Bcl-2 family protein A1/Bfl-1 regulates neutrophil survival and homeostasis and is controlled via PI3K and JAK/STAT signaling. *Cell Death Dis.* 7:e2103. https://doi.org/10.1038/cddis.2016.23

Vivier, E., D.H. Raulet, A. Moretta, M.A. Caligiuri, L. Zitvogel, L.L. Lanier, W.M. Yokoyama, and S. Ugolini. 2011. Innate or adaptive immunity? The example of natural killer cells. *Science.* 331:44–49. https://doi.org/10.1126/science.1198687

Vivier, E., D. Artis, M. Colonna, A. Diefenbach, J.P. Di Santo, G. Eberl, S. Koyasu, R.M. Locksley, A.N.J. McKenzie, R.E. Mebius, et al. 2018. Innate Lymphoid Cells: 10 Years On. *Cell.* 174:1054–1066. https://doi.org/10.1016/j.cell.2018.07.017

Vizcaíno, J.A., A. Csordas, N. Del-Toro, J.A. Dianes, J. Griss, I. Lavidas, G. Mayer, Y. Perez-Riverol, F. Reisinger, T. Ternent, et al. 2016. 2016 update of the PRIDE database and its related tools. *Nucleic Acids Res.* 44: 11033. https://doi.org/10.1093/nar/gkw880

Weber, G.F., B.G. Chousterman, S. He, A.M. Fenn, M. Nairz, A. Anzai, T. Brenner, F. Uhle, Y. Iwamoto, C.S. Robbins, et al. 2015. Interleukin-3 amplifies acute inflammation and is a potential therapeutic target in sepsis. *Science.* 347:1260–1265. https://doi.org/10.1126/science.aaa4268

Wicks, I.P., and A.W. Roberts. 2016. Targeting GM-CSF in inflammatory diseases. *Nat. Rev. Rheumatol.* 12:37–48. https://doi.org/10.1038/nrrheum.2015.161

Wipke, B.T., and P.M. Allen. 2001. Essential role of neutrophils in the initiation and progression of a murine model of rheumatoid arthritis. *J. Immunol.* 167:1601–1608. https://doi.org/10.4049/jimmunol.167.3.1601

Wipke, B.T., Z. Wang, W. Nagengast, D.E. Reichert, and P.M. Allen. 2004. Staging the initiation of autoantibody-induced arthritis: a critical role for immune complexes. *J. Immunol.* 172:7694–7702. https://doi.org/10.4049/jimmunol.172.12.7694

Yamin, R., O. Berhani, H. Peleg, S. Aamar, N. Stein, M. Gamliel, I. Hindi, A. Scheiman-Elazary, and C. Gur. 2019. High percentages and activity of synovial fluid NK cells present in patients with advanced stage active Rheumatoid Arthritis. *Sci. Rep.* 9:1351. https://doi.org/10.1038/s41598-018-37448-z

Yoshimura, A., T. Ohkubo, T. Kiguchi, N.A. Jenkins, D.J. Gilbert, N.G. Copeland, T. Hara, and A. Miyajima. 1995. A novel cytokine-inducible gene CIS encodes an SH2-containing protein that binds to tyrosine-phosphorylated interleukin 3 and erythropoietin receptors. *EMBO J.* 14:2816–2826. https://doi.org/10.1002/j.1460-2075.1995.tb07281.x

Zhu, Q., and T.D. Kanneganti. 2017. Cutting Edge: Distinct Regulatory Mechanisms Control Proinflammatory Cytokines IL-18 and IL-1β. *J. Immunol.* 198:4210–4215. https://doi.org/10.4049/jimmunol.1700352

Zitti, B., and Y.T. Bryceson. 2018. Natural killer cells in inflammation and autoimmunity. *Cytokine Growth Factor Rev.* 42:37–46. https://doi.org/10.1016/j.cytogfr.2018.08.001

Supplemental material

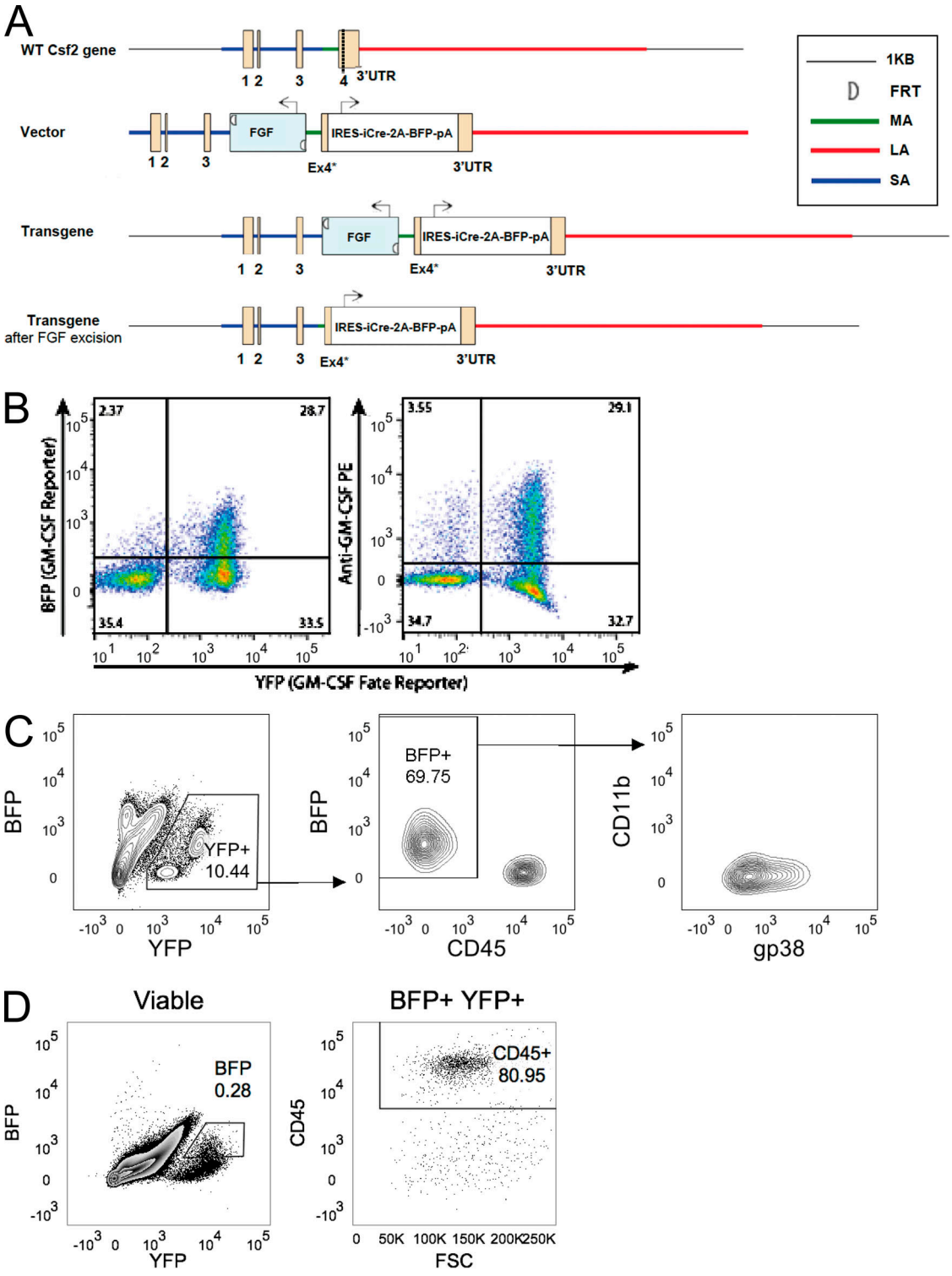

Figure S1. **Characterization of Gr/fr mice. (A)** Gr/fr mice were generated by targeted integration, resulting in replacement of WT GM-CSF gene (*Csf2*) with the vector. The IRES-iCre-2A-BFP-SV40pA cassette was placed 25 bp after the STOP codon in exon 4, in the 3′ untranslated region (UTR) of the *Csf2*. The FRT-flanked Neo cassette (FRT-Neo-FRT) was placed 330 bp upstream of exon 4 in intronic sequence and was later excised through breeding with FLP transgenic mice. The SA extends 2.1 kb 5′ to the Neo cassette and the LA 6.2 kb 3′ to the IRES-iCre-2A-BFP-SV40pA cassette. Length in bps: SA, 2,085; Neo, 1,561; middle homology arm (MA), 466; IRES-iCre-2A-BFP, 2,686; LA, 6,620. The transgenic construct has been designed to provide normal expression of GM-CSF, driven by natural controlling elements of *Csf2*. GM-CSF induction triggers the expression of iCre and BFP, given that BFP is downstream of iCre, all BFP$^+$ cells should also be iCre$^+$. These mice were then crossed Rosa26eYFP to enable lineage tracing via iCre-mediated YFP expression. **(B)** Naive CD4$^+$ T cells were isolated from Gr/fr mice mice and cultured in Th17 polarizing conditions and analyzed by flow cytometry comparing BFP reporter signal to intracellular staining of GM-CSF. **(C)** Flow-cytometric analysis of GM-CSF–producing cells (BFP$^+$ YFP$^+$) in the lung of naive Gr/fr mice. **(D)** Flow-cytometric analysis of GM-CSF–producing cells (BFP$^+$ YFP$^+$) in the joints of arthritic Gr/fr mice.

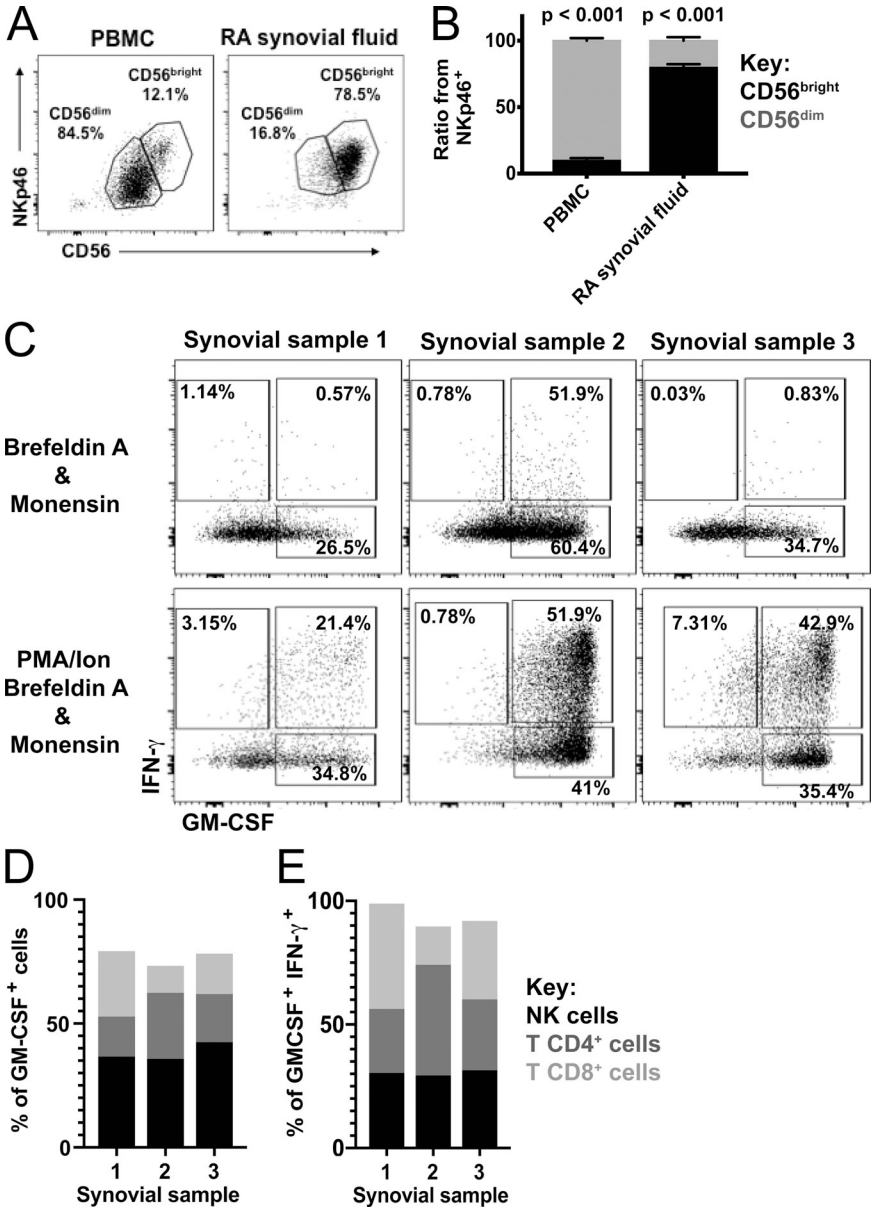

Figure S2. **Human NK cells produce GM-CSF in RA SF. (A and B)** FACS (A) and bar plots (B) showing the relative frequency of NK cell subsets (immature $CD56^{bright}$ and mature $CD56^{dim}$) in PBMCs from healthy donors or RA SF. Vertical bars, mean ± SEM, *n* = 3 donors. **(C)** FACS plots showing intracellular GM-CSF and IFN-γ staining of viable lineage$^-$ $CD7^+$ cells in RA SF. **(D and E)** Ratio of NK ($CD3^+$ $NKp46^+$), $CD4^+$ T cells ($CD3^+$ $CD4^+$) and $CD8^+$ T cells ($CD3^+$ $CD8^+$) populations among the $GM\text{-}CSF^+$ cells (D) or among the $GM\text{-}CSF^+IFN\text{-}\gamma^+$ cells from RA SF cells as in C.

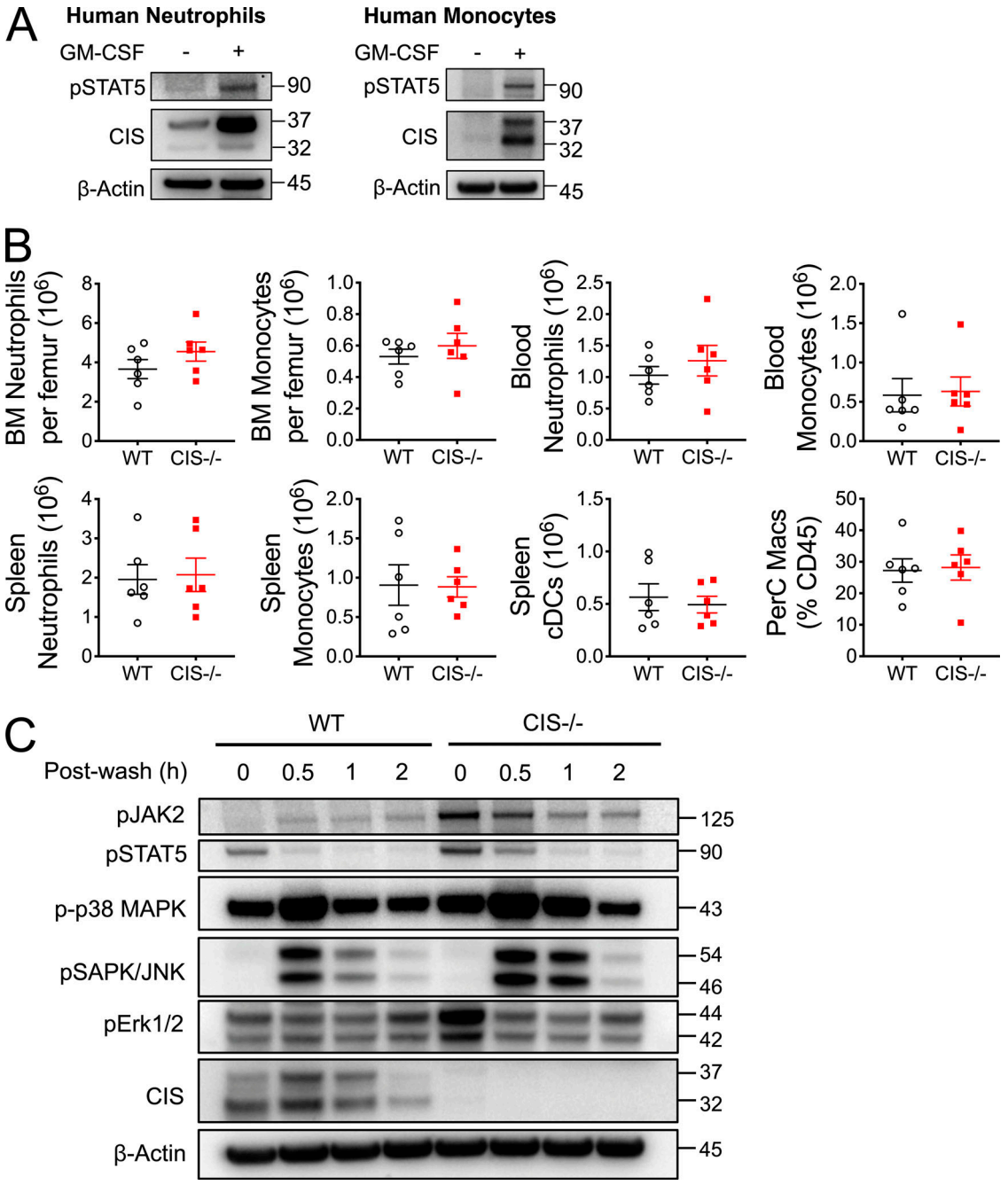

Figure S3. **Characterization of CIS-deficient myeloid cells. (A)** Immunoblotting of pSTAT5, CIS, and β-actin in human blood neutrophils and monocytes from healthy donors treated with GM-CSF. One experiment representative of three independent experiments with similar results. **(B)** Flow-cytometric analysis of myeloid cell populations in the BM, blood, spleen, and peritoneal cavity of naive WT and CIS$^{-/-}$ mice (n = 6 mice from one experiment, SEM). **(C)** Immunoblot analysis for pJAK2, pSTAT5, p-p38 MAPK, pSAPK/JNK, pErk1/2, CIS, and β-actin of WT or CIS$^{-/-}$ BM neutrophils primed with GM-CSF and washed free of cytokine-containing media before lysis at various times after wash. One experiment representative of three independent experiments with similar results. cDC, conventional dendritic cell.

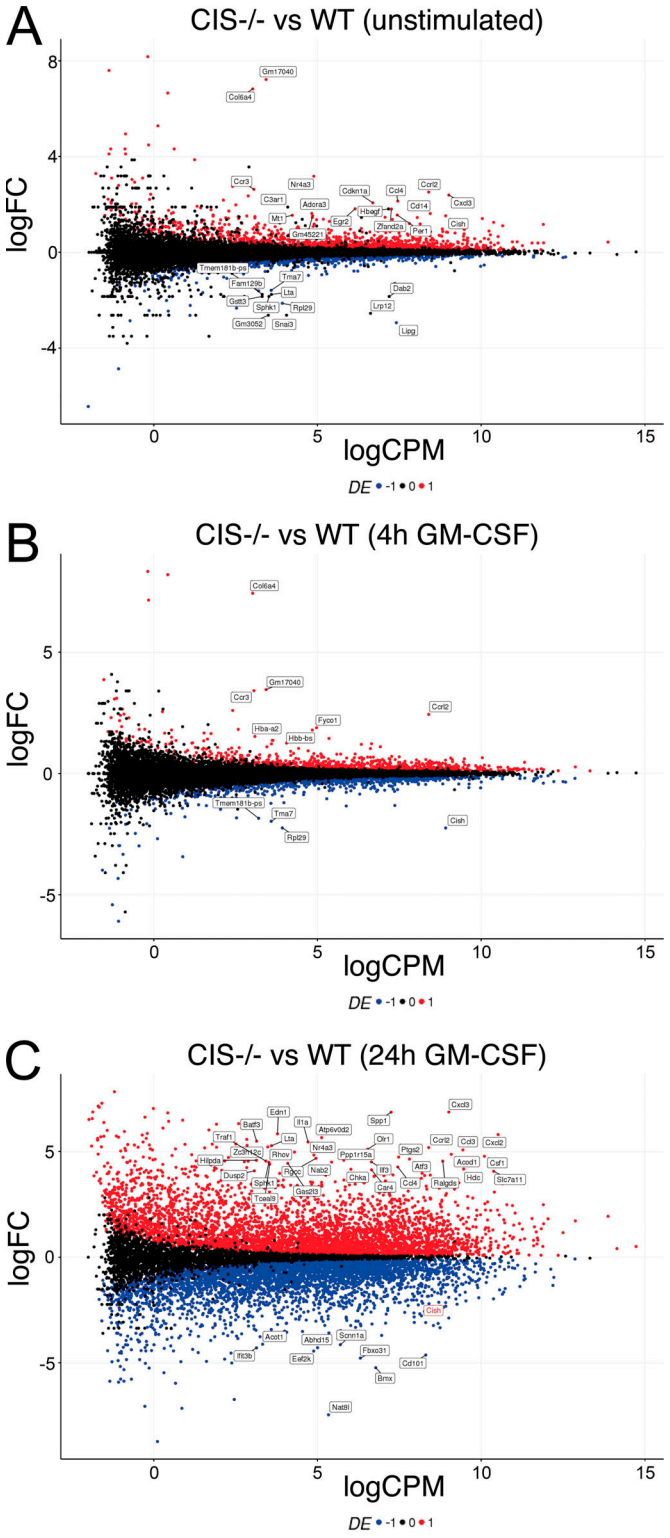

Figure S4. **RNASeq analysis of WT and CIS$^{-/-}$ neutrophils. (A–C)** MD plots showing log-fold change (CIS$^{-/-}$ vs. WT) and average abundance of genes for the corresponding RNASeq in BM neutrophils following isolation (A, unstimulated), or cultured in GM-CSF-containing media for 4 h (B) or 24 h (C). Significant differentially expressed (absolute $\log_2$ FC ≥ 1, FDR ≤ 0.05) genes are colored red (up-regulated) or blue (down-regulated).

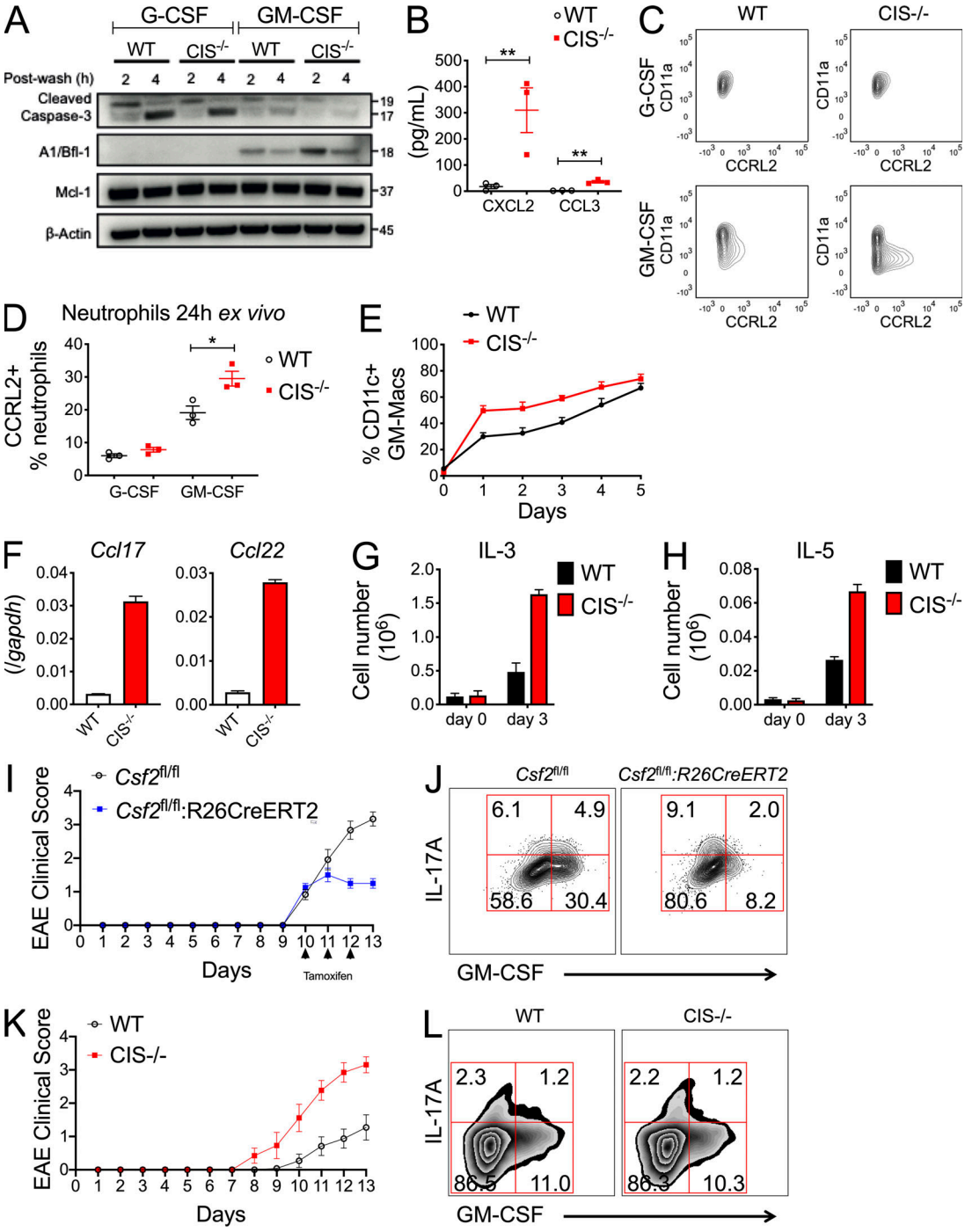

Figure S5. **CIS-deficiency confers hyperactivation of GM-CSF–driven responses in myeloid cells in vitro and in EAE. (A)** Immunoblot analysis for cleaved caspase-3, A1/Bfl-1, Mcl-1, or β-actin of WT or CIS$^{-/-}$ BM neutrophils stimulated with GM-CSF and washed free of cytokine-containing media before lysis at various times after wash. One experiment representative of three independent experiments with similar results. **(B)** CXCL2 and CCL3 analyzed by ELISA in culture supernatant of BM neutrophils from WT and CIS$^{-/-}$ mice following stimulation with GM-CSF for 24 h (n = 3 mice from one experiment, SEM). **(C and D)** Flow-cytometric analysis of CCRL2 and CD11a surface expression on G-CSF or GM-CSF–stimulated BM neutrophils from WT or CIS$^{-/-}$ mice. **(D)** Data are expressed as percentage of neutrophils (n = 3 mice from one experiment, SEM). **(E)** Frequency of CD11c^{+} GM-Macs in GM-CSF–stimulated BM monocytes from WT and CIS$^{-/-}$ mice at indicated times (n = 4 mice pooled from two independent experiments, SEM). **(F)** Expression of mRNA for GM-CSF–inducible chemokines (*Ccl17* and *Ccl22*) by BM monocytes analyzed by real-time PCR, normalized to *Gapdh*, at 8 h after stimulation with GM-CSF (n = 3 mice from one experiment, SEM). **(G)** Flow-cytometric analysis of WT and CIS$^{-/-}$ BM common myeloid progenitor cells upon culture in IL-3 for 3 d (n = 3 mice from one experiment, SEM). **(H)** Flow-cytometric analysis of WT and CIS$^{-/-}$ BM eosinophils upon culture in IL-5 for 3 d (n = 3 mice from one experiment, SEM). **(I)** EAE development in *Csf2*$^{fl/fl}$ and *Csf2*$^{fl/fl}$:R26CreERT2 mice with tamoxifen treatment after EAE onset (n = 12 mice pooled from two independent experiments, SEM). **(J)** Representative intracellular GM-CSF and IL-17A staining of CD4 T cells in the CNS of *Csf2*$^{fl/fl}$ and *Csf2*$^{fl/fl}$:Ncr1-Cre mice with EAE following tamoxifen treatment as in I. **(K)** EAE development in WT and CIS$^{-/-}$ mice (n = 12 mice pooled from two independent experiments, SEM). **(L)** Representative intracellular GM-CSF and IL-17A staining of CD4 T cells in the CNS of WT and CIS$^{-/-}$ mice with EAE as in K. *, P < 0.05; **, P < 0.01.

Table S1 is provided online and shows reagents.